CHAPTER EIGHT

Macroscopic pedestrian dynamics modelling

Cecile Appert-Rolland[a,*] **and Alethea B.T. Barbaro**[b]
[a]University Paris-Saclay, CNRS, IJCLab (UMR 9012), Orsay, France
[b]Delft Institute of Applied Mathematics, Delft University of Technology, The Netherlands
*Corresponding author. e-mail address: cecile.appert-rolland@ijclab.in2p3.fr

Contents

Abstract

The dynamics of pedestrian crowds can involve very different scales. While situations involving only a few pedestrians are better described by microscopic models, large crowds can exhibit collective behavior which can be captured by macroscopic equations. Macroscopic models describe crowds as fluids of pedestrians, where individuals cannot be distinguished anymore. This fluid is characterized by some local averages of pedestrian density and velocity. These macroscopic variables are shown to obey conservation equations, which can be solved using the method of characteristics. In contrast with classical fluid equations, the evolution of density and velocity depends on some target or preferred velocity that can be specific to different pedestrian groups. We review the advantages and drawbacks of these conservation laws adapted to the pedestrian case. We also discuss the associated numerical methods, which can be Eulerian or Lagrangian. Particular attention will be devoted to the link between models

Advances in Transport Policy and Planning, Volume 15
ISSN 2543-0009, https://doi.org/10.1016/bs.atpp.2025.04.004

at microscopic, mesoscopic, and macroscopic scales. Using macroscopic approaches give access to a whole set of methods developed for this kind of partial differential equation, including the study of phase transition, or of travelling waves. Eventually, recent variants that have been proposed in the literature will be outlined.

1. Introduction

A lot of research has been devoted to interactions between a few individual pedestrians. But there is an increasing interest in understanding the global dynamics of crowds, taken as a whole. Indeed, more and more large scale events occur (concerts, sport, cultural, or religious events, etc), and there is a need to be able to monitor these large crowds in order to limit the risk of accidents (Feliciani et al., 2023; Haghani et al., 2023).

Simulating large crowds is needed for the design of facilities that allow for fast evacuation, while avoiding high density congestion points. Simulations can also serve as a basis for real-time control of entry fluxes into the facility. As soon as the number of pedestrians becomes large, agent-based simulations are out of reach or too time-consuming. By contrast, describing the crowd as a fluid allows to diminish a lot the number of degrees of freedom. Only the density and velocity fields have to be determined.

We will address in this chapter the so-called macroscopic modelling approach, which was for a large part inspired by fluid mechanics. After a presentation of the various families of macroscopic models, we shall discuss how the various levels of descriptions - micro, meso, macroscopic - can be related. We shall then present how specific features like granularity, heterogeneity or anticipative behavior can be taken into account. Various numerical methods applicable to macroscopic models will be presented, before the final discussion.

2. Conservation laws

In the XVIIIth century, Antoine de Lavoisier claimed about matter that ≪ Rien ne se perd, rien ne se crée, tout se transforme ≫ (“Nothing is lost, nothing is created, everything is transformed”). This statement can be expressed in mathematical form by so-called conservation laws, which are partial differential equations. Let’s consider a quantity - let’s say R to be

generic - that is conserved, and let ρ be its density. Being conserved does not mean that there is always the same amount of it in the system, but that we can track any change/input/output of it.

The general form of a conservation law is

$$\partial_t \rho + \nabla . \mathbf{F}(\rho) = \text{source - sink terms} \tag{1}$$

where $\mathbf{F}(\rho)$ is the flux of the quantity Q per surface unit at any point in space and time, and the right-hand side stands for bulk sources and sinks for the quantity R.

It becomes more clear why the previous equation expresses the conservation of R, when it is integrated on a volume $\mathcal{V}$. It becomes then

$$\begin{aligned} &\frac{d}{dt}\begin{bmatrix}\text{Total amount}\\ \text{of R}\\ \text{in volume } \mathcal{V}\end{bmatrix} - \begin{bmatrix}\text{Flux of R}\\ \text{entering } \mathcal{V}\\ \text{through boundary}\end{bmatrix} + \begin{bmatrix}\text{Flux of R}\\ \text{exiting } \mathcal{V}\\ \text{through boundary}\end{bmatrix} \\ &= \begin{bmatrix}\text{Total amount}\\ \text{of R produced}\\ \text{in the bulk of } \mathcal{V}\\ \text{per unit time}\end{bmatrix} - \begin{bmatrix}\text{Total amount}\\ \text{of R removed}\\ \text{in the bulk of } \mathcal{V}\\ \text{per unit time}\end{bmatrix} \end{aligned} \tag{2}$$

Indeed the variations of the total amount of R inside volume $\mathcal{V}$ are due to the difference between inputs or outputs of R, either in the bulk or through the boundaries.

Let us take as an example a pedestrian commercial street. Pedestrians cannot be spontaneously created, or cannot disappear suddenly through a magic charm. Their number is thus a conserved quantity. The total number of pedestrians in the street varies depending on how many pedestrians enter or exit the street. Pedestrians may enter/exit the street not only at street ends (corresponding to boundary conditions in the model), but also in the bulk when they enter or exit shops or restaurants (sink or source terms in the model).

However for simplicity, in the remaining of the paper, we shall ignore these bulk source/sink terms which are important in rather specific situations, in order to concentrate on the dynamics of the crowd itself.

To go further, it is informative to compare crowds with fluids, for which not only mass but also momentum is conserved, allowing to write two conservation equations (the so-called Navier-Stokes equations). By contrast, as pedestrians or cars are in contact with the road, they do not conserve momentum. Only mass (or rather, agents' number) is conserved. We express this through an equation for the density $\rho(\mathbf{x}, t)$, which for the

remainder of the chapter represents the density of pedestrians or cars at point $\mathbf{x}$ in space and time t. The density therefore obeys the following conservation equation

$$\partial_t \rho(\mathbf{x}, t) + \nabla \cdot \mathbf{F}[\rho(\mathbf{x}, t)] = 0 \tag{3}$$

as we ignore sink and source terms.

We have only one Eq. (3) for two unknowns: the density $\rho(\mathbf{x}, t)$ and the associated flux $\mathbf{F}$. If we are to solve this equation, we need to close it with another relation.

2.1 First-order models

We will first consider so-called first-order models, where the adaptation in velocity to the surrounding density is immediate and acceleration is not explicitly included in the pedestrian model.

2.1.1 Fundamental diagrams

One first solution in order to get a closed form for Eq. (3) is to provide a relation between $\mathbf{F}$ and ρ. Actually, the way we wrote Eq. (3) was already assuming that $\mathbf{F}$ was a function of ρ and only ρ. This assumption is not completely obvious a priori. It comes mainly from car traffic, where traffic engineers have measured extensively the so-called fundamental diagram, namely the $F(\rho)$ relation (for cars, one can consider that the flow is uni-dimensional, and thus F is a scalar).

And indeed, some general forms have been inferred from the data. Fig. 1-left and 1-middle present two examples of fundamental diagrams (FDs) that are often used in car traffic, the triangular and Greenshield's ones (Kühne, 2011). Of course these are idealized relations, but they capture most important features. In both cases, the flux is quasi-linear at small density (free flow state), increases up to a maximum called the capacity, and then decreases with density (congested state) up to complete blockage. Once Eq. (3) is complemented with such a relation $F(\rho)$, it has a closed form that can be solved, as we shall see in Section 2.1.2.

For pedestrians, many geometries of flows can be considered, not necessarily one-dimensional or uni-directional. It turns out that finding a universal form for the fundamental diagram is out of reach, as pedestrian FDs are more situation dependent than for cars. We refer the reader to Chap. 3 for further discussion. Note also that we have presented the fundamental diagram under its form $F(\rho)$ but it can as well be defined in terms of an average velocity $V(\rho) \equiv F(\rho)/\rho$.

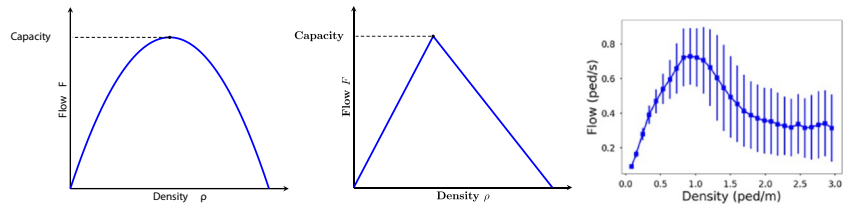

Fig. 1 Fundamental diagrams showing flow as a function of density: left and middle show idealized FDs used in the context of car traffic. The maximal value of the flow is called capacity. (left) Greenshield; (middle) Triangular; (right) Experimental FD obtained for pedestrians walking in line. *Obtained from the data of Jelić et al. (2012), for individual measurements.*

Here we shall in a first stage focus on one-dimensional unidirectional fundamental diagrams, as shown on Fig. 1-right. Though we can still distinguish a free flow and a congested phase, we immediately see a difference with cars: while the velocity of cars quite rapidly drops to zero, pedestrians manage to move even at very high density. Indeed they are able to deform their body and to squeeze through others, at densities that oblige them to have physical contact with their neighbors. Nevertheless, whatever the relation between flux and density is, the structure of the equations and the way to solve them is always the same, as we shall see now.

2.1.2 Mathematical aspects (method of characteristics, shockwave theory, etc.)

In this section we present how one can solve the system given by Eq. (3) and the relation $F(\rho)$, in the case of a one-dimensional one-directional flow:

$$\partial_t \rho(x,\, t) + \partial_x F(\rho(x,\, t)) = 0 \tag{4}$$

In the context of car traffic, this is called the LWR model (Lighthill and Whitham, 1955), but the same structure is met for one dimensional unidirectional pedestrian flows.

As a preliminary calculation, let us consider a curve in the spatio-temporal space defined under a parametric form $(X(t),\, t)$. The evolution of ρ along this curve is given by the material derivative (also called total derivative)

$$\frac{d\rho(X(t),\, t)}{dt} = \partial_t \rho(x,\, t) + \frac{dX}{dt}\, \partial_x \rho(x,\, t) \tag{5}$$

This expression will become identical to the left-hand side of Eq. (4) provided that we choose $X(t)$ such that

$$\frac{dX}{dt} = F'(\rho(x,\, t)). \tag{6}$$

Once integrated from a specific initial or boundary condition, Eq. (6) defines a curve $(X(t),\ t)$ (called *characteristics*). Along this curve, the material derivative of ρ is zero, as stated in Eq. (4), and thus ρ is constant all along the curve. From Equation (6), we see that the characteristics curve has a slope $F'(\rho(x,\ t))$ which, as it depends only on density, must itself be constant along the curve $(X(t),\ t)$. Characteristics are thus straight lines for the LWR equation (4) considered here.

Fig. 2 illustrates how the knowledge of density in the initial state can be transported along a characteristics (dashed-dotted curves). Characteristics should not be confused with the trajectories of the agents – cars or pedestrians – (solid lines in Fig. 2-top), though they may coincide in free flow if the free velocity is constant.

An important property is that $F'(\rho) = V(\rho) + \rho V'(\rho) \leq V(\rho)$, meaning that information about the density always propagates more slowly than individuals. Seen from the point of view of a pedestrian, this means that information cannot come from their back. This is a good feature as pedestrians react mostly to what happens in front. In the congested phase, information even propagates backwards, as in the example of Fig. 2-top-right.

In order to understand the behavior of these models, it is helpful to solve it in a simple situation, namely a Riemann Problem (Haberman, 1998; Toro, 2009; Ketcheson et al., 2020): as illustrated in Fig. 3, the initial state of the system consists in two constant density regions separated by a discontinuity. There will be two families of characteristics emitted from this initial state, with slopes respectively $F'(\rho_L)$ and $F'(\rho_R)$. Depending on the initial densities, several cases may occur. If $F'(\rho_L) > F'(\rho_R)$, as shown in Fig. 3-Top, the two families of characteristics would cross each other. This is not possible as density cannot take at the same time the value of the left and of the right initial density. Instead, a shock is formed, that separates the two regions. The speed of the shock s simply stems out from mass conservation

$$s = \frac{F'(\rho_L) - F'(\rho_R)}{\rho_L - \rho_R} \tag{7}$$

If $F'(\rho_L) < F'(\rho_R)$, the two families of characteristics would rather separate from each other, giving rise to a rarefaction wave (see Fig. 3-Bottom).

In general, initial conditions are more complex and give raise to non straight shock trajectories, as shown for example in Fig. 4. The shock speed

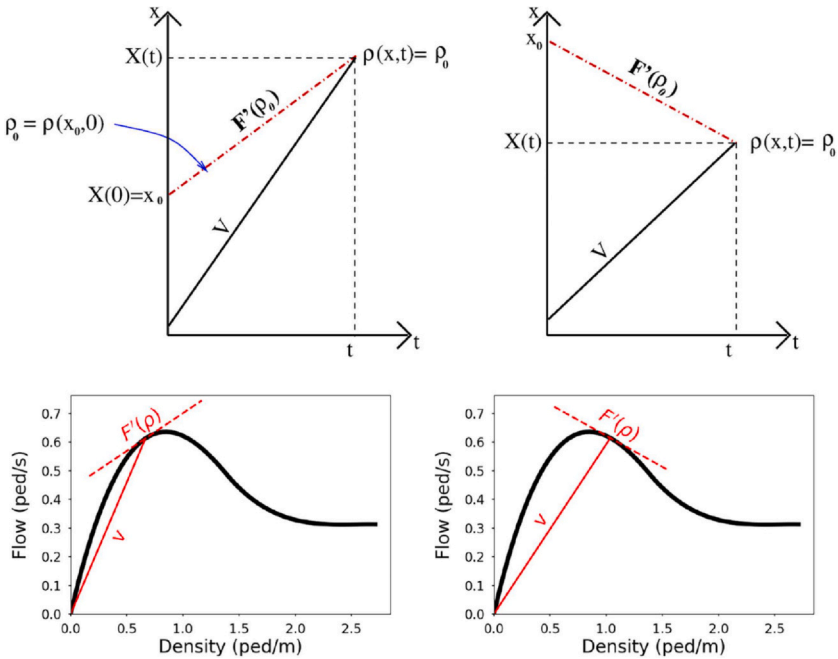

Fig. 2 Top: sketched spatio-temporal plots in free flow (left) or congested (right) states. The spatial coordinate is vertical and the time horizontal so that the slope of the characteristics $F'(\rho)$ can be directly taken from the fundamental diagram below. The characteristics which goes through the position x of the pedestrian at time t ($X(t) = x$) is represented with a red dashed-dotted line. Characteristics propagate downstream (resp. upstream) in free-flow (resp. congested) state. The solid line shows the trajectory of the individual agents arriving in $X(t) = x$ at time t. Bottom: fundamental diagrams and graphical representation of the speed $F'(\rho)$ of characteristics (given by the slope of the tangent to the FD - thin dashed red line), and the speed v of individuals (slope of the thin solid red line). In the free-flow phase (left), the characteristics speed is positive, while in the congested phase (right) it is negative.

however always obeys locally Eq. (7), as mass conservation still holds. More details on the method of characteristics can be found in many textbooks, for example in (Haberman, 1998; Toro, 2009; Ketcheson et al., 2020).

In particular, it should be noted that the weak solutions (ie with discontinuities) of equation (4) are not unique - as in general for scalar conservation laws (Evans, 1998). In the case of fluids, one solution can be selected as the physical one, using the fact that at small scale, the shock is regularized by viscosity. In the case of pedestrians, it can be discussed whether such condition still holds. On the one hand, some similar selection criterion has been derived through micro-macro derivation in the context

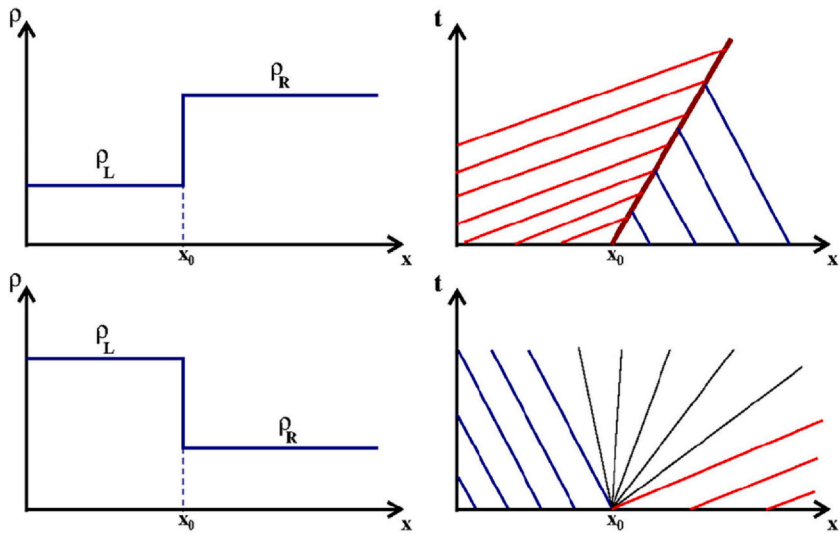

Fig. 3 Left: initial conditions of Riemann problems. Density is constant on both sides of a discontinuity. Right: corresponding spatio-temporal plots with characteristics. Top: propagation of a shock between two families of convergent characteristics. Bottom: rarefaction wave separating two families of divergent characteristics.

of a follow-the-leader model (Francesco et al., 2017). On the other hand, the possibility to have non-classical shocks – meaning shocks that do not obey entropic arguments - was sometimes used to provide the model with new properties (Colombo and Rosini, 2005).

2.1.3 Multi-directional flows

Until now, we considered only one-dimensional one-directional pedestrian flows, so that all individuals had the same goal. Actually, pedestrians with different destinations can share the same space. Let us consider for example the case of a bi-directional flow in a corridor. In this case, we have to distinguish two types of pedestrians, going to the left or to the right, with respectively density ρ_+ and ρ_-.

A simple extension of the LWR model to two species consists in writing two coupled mass conservation equations, one for each of the pedestrian families

$$\begin{aligned} \partial_t \rho_+(x,\, t) + \partial_x f\,(\rho_+,\, \rho_-) &= 0 \\ \partial_t \rho_-(x,\, t) + \partial_x f\,(\rho_-,\, \rho_+) &= 0 \end{aligned} \tag{8}$$

Note that now, the flux $f(\cdot,\, \cdot)$ depends not only on the density of pedestrians going in the same direction as the population under consideration

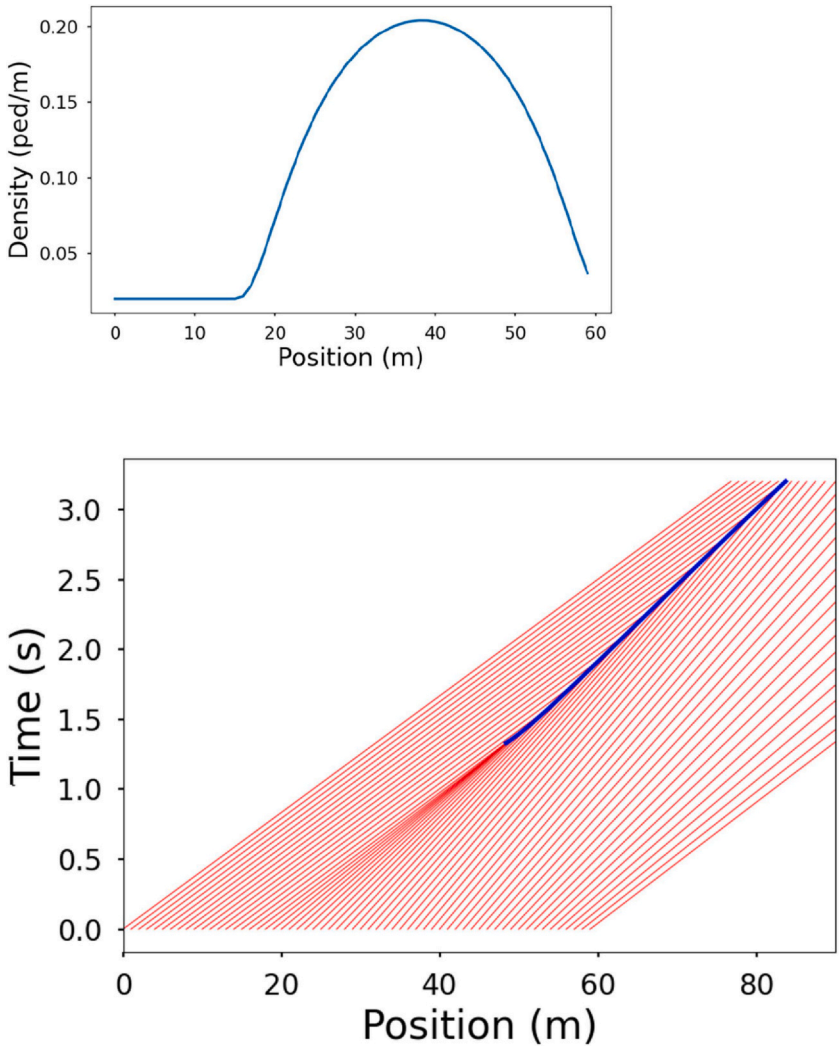

Fig. 4 Top: initial density profile. Bottom: characteristics (thin -red online- lines) and the resulting shock (thick -blue online- line).

(the first variable of the function f), but also on the density of oppositely going ones (the second variable). This flux function can be measured experimentally, as shown in Fig. 5 in the case of a bi-directional flow in a ring corridor (Motsch et al., 2018). A fit, here by a second-order

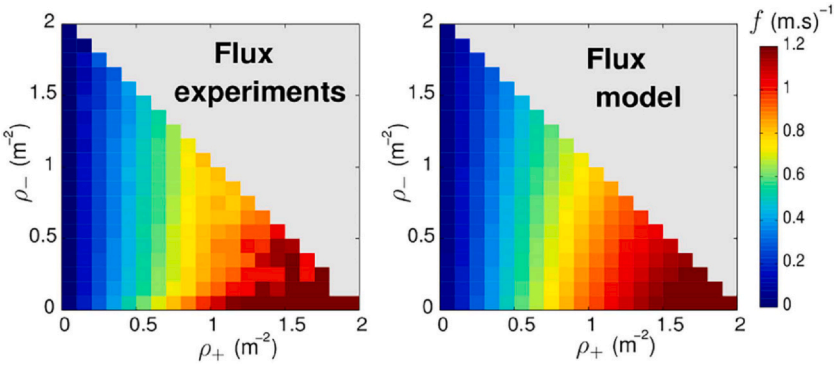

Fig. 5 Fundamental diagram for a one-dimensional bi-directional flow. Left: experimental data. Right: polynomial fit. The flux is given in pedestrians per second and per unit of corridor width. *From Motsch et al. (2018).*

polynomial in ρ_+ and ρ_-, provides an analytical expression for f which can be used to complement Eq. (8).

We have now a full model that can be used for simulations. Let us compare how it predicts the bulk dynamics, again in the case of the bi-directional corridor. If we consider the initial and boundary conditions as given by the experimental observations, it is then possible to use the macroscopic model of Eq. (8) to simulate the behavior of the crowd in the bulk. A comparison with direct observation shows that the model is indeed able to reproduce the propagation of dense regions within the crowd (see Fig. 6).

2.1.4 Bi-dimensional models

Until now, we have considered only models in one dimension, which would be relevant in special settings as corridors. But in general, pedestrians move in a two dimensional space.

An important model was proposed in 2002 by Hughes (2002). It relies again on the mass conservation equation (3). Again one can assume that the speed or flux of the pedestrians at a given point is given by a fundamental diagram $|\mathbf{F}| = F(\rho)$. But now, not only the modulus but also the direction of the flow must be specified.

It is reasonable to assume that pedestrians want to minimize their travel time to some goal they want to reach. The velocity of pedestrians will thus be assumed to be aligned with the gradient of some potential measuring the travel time from each location. Note that this travel time may take into account not only the distance to the goal, but also the possible congestions.

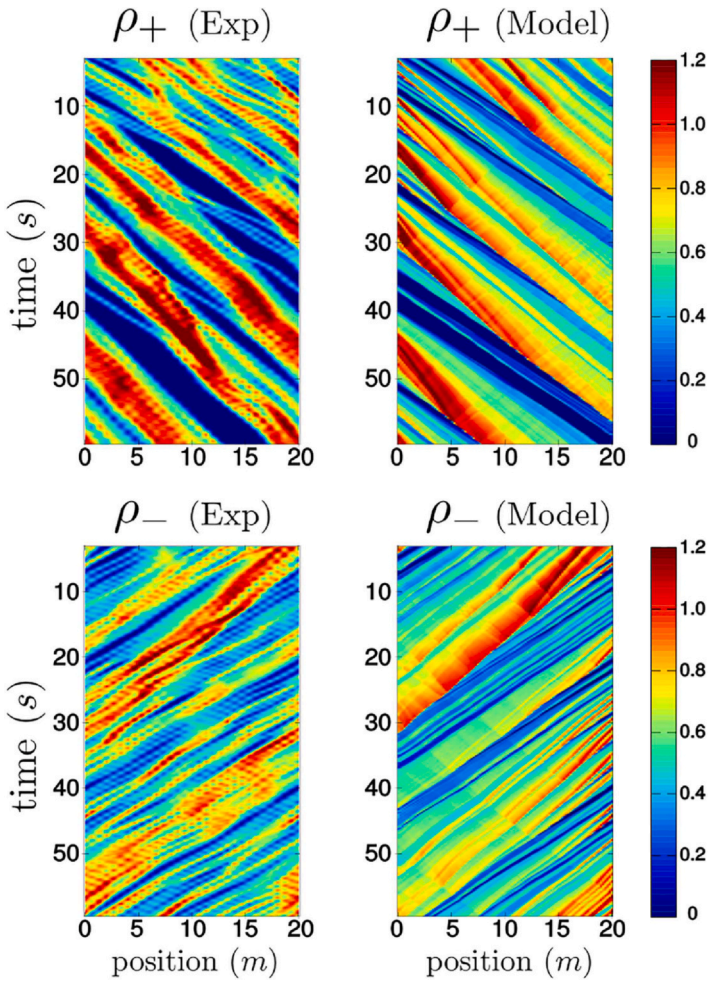

Fig. 6 Spatio-temporal plot of the density field in a one-dimensional bi-directional flow. Left: experimental data. Right: simulation results. *From Motsch et al. (2018).*

We express it according to the formulation proposed in (Xia et al., 2009; Huang et al., 2009) for which mass conservation (3) is complemented by

$$\frac{\mathbf{F}}{|\mathbf{F}|} = -\frac{\nabla\phi}{|\nabla\phi|} \tag{9}$$

with potential ϕ obtained from the Eikonal equation

$$|\nabla\phi| = C\left(\rho\left(\mathbf{x},\, t\right),\, \mathbf{x},\, t\right) \tag{10}$$

where C is some local cost per traveled distance. If $C = 1$ everywhere in the walkable domain, only the distance to the exit will be taken into account. But the interesting feature of Hughes' model and derivatives is precisely to rather take a density dependent function for C (Di Francesco et al., 2011). Fig. 7 gives an example of such a potential ϕ. We see clearly how the gradient of this potential will be globally oriented towards the exits, while some local detours may be induced by locally congested areas (Huang et al., 2009).

Hughes' model poses a lot of mathematical questions (Amadori et al., 2023). In particular, the flow field obtained from shortest travel times might be discontinuous. Think of a room with two exits, there will be a sharp separation between those taking one exit or the other. This poses mathematical difficulties and some non-classical shocks may arise, which

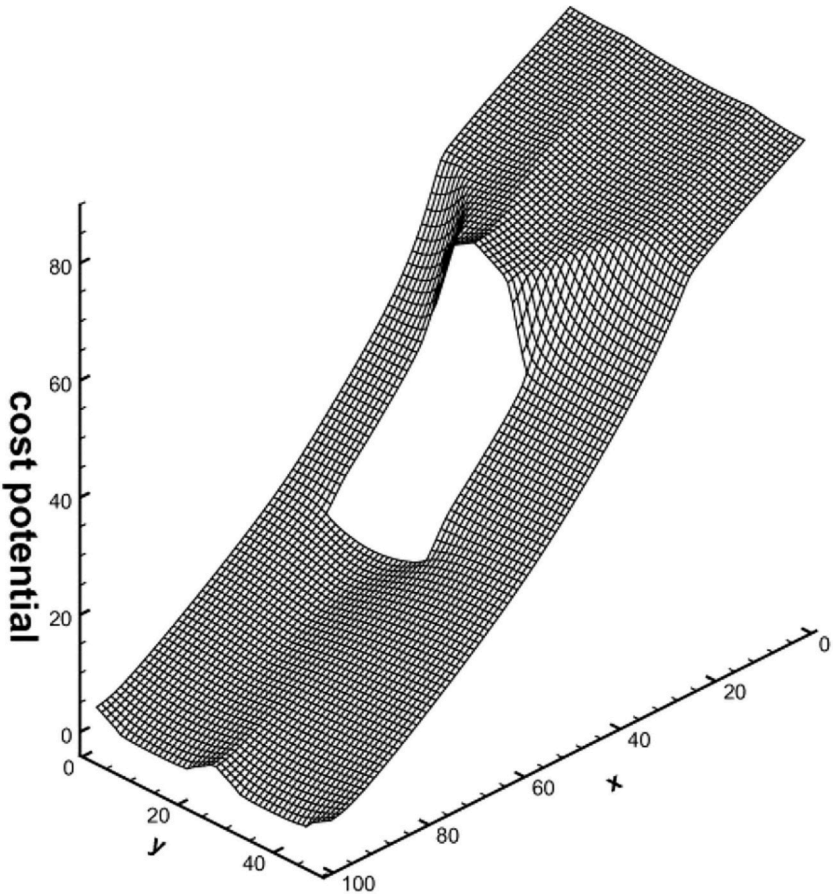

Fig. 7 Example of a potential ϕ at a given time in the case of a platform with an obstacle in the middle, and 2 exits at location $x = 100$. *From Huang et al. (2009).*

have non-local origin (Amadori and Francesco, 2012; Andreianov et al., 2023). One possible solution is to add some diffusive term to blur these discontinuities (Di Francesco et al., 2011; Carlini et al., 2017; Herzog et al., 2023). On the other hand, when restricted to one dimension, this model can be reduced to coupled LWR equations as in Eq. (8).

2.1.5 Advantages and limitations of first-order models

In spite of their simplicity, first-order models can describe several features of traffic, namely congestion formation or dissolution of queues (Goatin, 2023). They rely however on some assumptions that it is important to be aware of.

First-order models assume that at each instant of time, the flow (or speed) is exactly the one given by the fundamental diagram, meaning that the speed immediately adapts to any change in the density. It is known that this is not true in real systems, for which reaction times or relaxation processes exist. Besides, this behavior implies an infinite braking and accelerating capacity, which is also obviously a strong assumption. This immediate adaption is the reason why first-order models are sometimes called 'equilibrium models". A consequence of this strong hypothesis is that the stop-and-go waves that form spontaneously in pedestrian flows (Lemercier et al., 2012; Fehrenbach et al., 2015; Helbing et al., 2007) are not described by first-order models, in particular by Hughes's model (Twarogowska et al., 2013).

Another limit (Colombo and Rosini, 2005) is that, as density is conserved along the characteristics, the maximal density in the system at a given time cannot be larger than the maximal density in the initial state or at the boundaries (Maximum Principle). By contrast, in real crowds, some situations can lead locally to very high densities and cause accidents.

Still, these models can be useful for crowd monitoring, as their simplicity allows for real time applications. Besides, they give an easy access to the physical understanding of various phenomena.

2.2 Second-order models

In second-order models, we acknowledge that pedestrians may not immediately adapt their speed to the current density, but that this is rather done through a relaxation process that takes some time. A second equation for the relaxation of velocity is thus written. Note however that there is no strong physical law that enforces the form of this equation such as mass conservation for the density equation.

The first proposal by (Payne, 1971; Whitham, 1974) for such a velocity equation in the context of car traffic were thus simply inspired by fluid

mechanics. But it was soon realized that unrealistic effects were obtained, such as negative velocities, and a paper entitled "Requiem for second-order fluid approximations of traffic flow" seemed to close this direction of research (Daganzo, 1995).

Indeed, a molecule arriving in a congested area would bounce back due to pressure, while a car or pedestrian would just slow down and wait until the way is cleared. This difference is due in particular to the fact that pedestrians or drivers observe the flow not from a fixed point on the side of the road, but from their own position. In mathematical terms, this can be expressed by the fact that agents do not react only to the spatial gradient of density, as a fluid would do, but rather to its material (or total) derivative. Aw & Rascle were the first ones to understood this point (Aw et al., 2002) and to propose a model including this material derivative, allowing for the "Resurrection" of this type of models (Aw and Rascle, 2000). A similar proposal was made by Zhang (Zhang, 2002). The ARZ model, proposed in the frame of vehicular traffic and thus one-dimensional, reads

$$\partial_t \rho + \partial_x(\rho v) = 0 \tag{11}$$

$$\partial_t v + v\partial_x v = -(\partial_t + v\partial_x)p(\rho) + \frac{1}{\tau}[V(\rho) - v] \tag{12}$$

In the first equation, which expresses the conservation of the number of agents, the flux $F = \rho v$ is now expressed in terms of the velocity v which evolves according to the second equation. The second equation has a form familiar froms that obtained in fluid mechanics from a combination of mass and momentum conservation. In traffic, however, conservation of momentum does not hold, but we keep a similar form with two significant changes. First the gradient of $p(\rho)$, sometimes called *pressure* in analogy with fluid mechanics, is replaced by a material derivative $\partial_t + v\partial_x$, as explained above. Additionally, the last term of Eq. (12) is a driving force towards the values prescribed by the fundamental diagram.

Another way to understand the second equation is to consider the quantity $w(x, t) = v(x, t) + p(\rho(x, t))$. In this case, equation (12) can be expressed as

$$(\partial_t + v\partial_x)w = \frac{1}{\tau}[V(\rho) - v].$$

As w is advected with particles, as seen by the use of the material derivative, it has been interpreted as a desired velocity. Then $p(\rho)$ can be interpreted as a velocity offset between the desired and real velocities, expressing how a

density increase can impede motion. The right-hand side is driving the velocity towards that dictated by the Fundamental Diagram through a relaxation process.

Note that though this family of models is called *second-order models*, the equations in fact only involve first-order derivatives. As suggested by (Aw and Rascle, 2000), it would thus be more appropriate to call these *two-equations models*.

2.2.1 Method of characteristics

Again this system of equations can be solved using the method of characteristics. The difference with the approach presented in Section 2.1.2 is that now, as we have 2 coupled equations to solve, we shall have 2 families of characteristic curves. Along each of these families, a specific combination of the variables ρ and v - the so-called Riemann invariants - will obey a conservation law.

The method of characteristics can thus be seen as a change of variables that allows to turn a system of two coupled Partial Differential Equations (PDEs) into Ordinary Differential Equations along the characteristics curves. The problem becomes in principle more easy to solve under this new form.

For the system (11)–(12) above, the Riemann invariants are v and $v + p(\rho)$ (Aw and Rascle, 2000). Each point of the x, t plane can be seen as the intersection of two characteristics, one of each family, which will prescribe the value of the Riemann invariants, from which the ρ and v values can be recovered.

In this special case, the Riemann invariant $v + p(\rho)$ is conserved along a family of curves that propagate with the same speed as individuals. In mathematical terms, this reads

$$(\partial_t + v\partial_x)[v + p(\rho)] = 0 \tag{13}$$

The quantity $v + p(\rho)$ is thus transported unchanged by the pedestrians themselves, and this is what allows to interpret it as a desired velocity.

An important property is that both families of characteristics propagate with a speed equal or inferior to the one of pedestrians (Aw and Rascle, 2000). So no information comes from behind. This requirement was not fulfilled in the original Payne-Whitham model (Payne, 1971; Whitham, 1974) and this is why it had unphysical properties.

2.2.2 Bi-directional flows

Again it is possible to adapt 2nd order models to the case of bi-directional flows. The number of equations is doubled as now they must be written for ρ_+ and ρ_- (Appert-Rolland et al., 2011; Degond et al., 2011). The main

difficulty is that, while for car traffic all vehicles drive in the same direction, here pedestrians walking in opposite directions may converge and create high density regions which, above a certain level, would be unphysical. It is thus important to enforce some density limitation, for example by adding a pressure-like term that diverges when density approaches the maximal threshold (Berthelin et al., 2008; Appert-Rolland et al., 2011; Dogbé, 2012). However it is then difficult to fully avoid numerical instabilities.

2.2.3 Second-order models in two dimensions

A second-order model in two dimensions adapted for pedestrians was first proposed by (Jiang et al., 2010). Mass conservation is complemented by an equation for the relaxation of the velocity, which is now the two-dimensional vector $\mathbf{v}$,

$$\partial_t \rho + \partial_x(\rho \mathbf{v}) = 0 \tag{14}$$

$$\partial_t \mathbf{v} + (\mathbf{v}\cdot\nabla)\mathbf{v} = -\nabla P(\rho) + \frac{1}{\tau}[\mathbf{V}(\rho) - \mathbf{v}] \tag{15}$$

The desired velocity is still computed from an Eikonal equation (see Eq. (10)) as for Hughes' model.

This model, as some later ones (Twarogowska et al., 2013), is a direct generalization of the Payne-Whitham model, and as such, it inherited of its properties, namely that pedestrians do not react only to what happens in front, but also in the rear, and that pedestrians can walk against the main flow in some cases (Jiang et al., 2010). Some two-dimensional extensions of the ARZ model have been proposed (Jiang et al., 2016), but possibly pedestrians still may react not only to the front but also to the rear (Jiang et al., 2022).

As in one-dimension, the addition of a diverging pressure when we approach the maximal density may allow to account for congestion effects (Aceves-Sánchez et al., 2024; Chaudhuri et al., 2023, 2024a, 2024b). Of course the numerical solution of two dimensional models is more complex than in one dimension, and a lot of efforts have been devoted in proposing appropriate numerical schemes (Jiang et al., 2010; Twarogowska et al., 2013; Jiang et al., 2022; Aceves-Sánchez et al., 2024). In contrast with first-order models, second-order models are able to display stop-and-go waves, as it occurs in real systems (Jiang et al., 2010; Twarogowska et al., 2013). Figs. 8 and 9 show such waves. The counterpart is that these models easily lead to instabilities (Appert-Rolland et al., 2011).

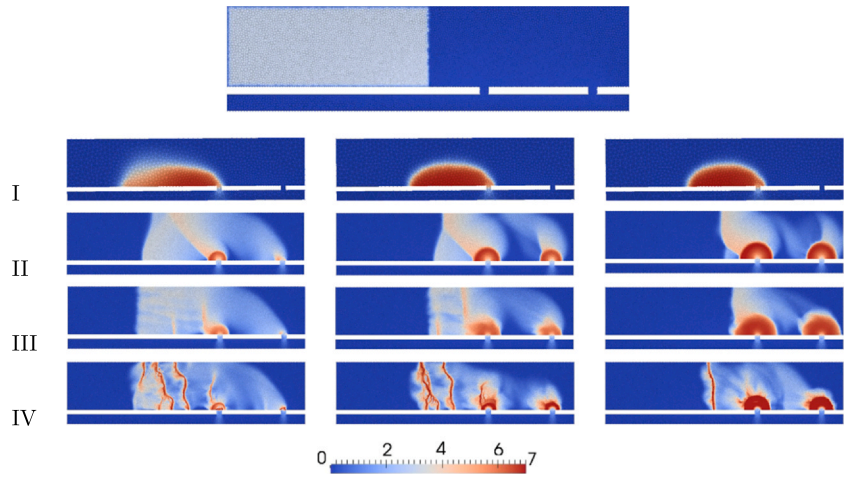

Fig. 8 Simulation of the evacuation of a room with two doors using various models. Top: density heatmap for the initial condition, with pedestrians uniformly distributed only over the left half of the room. Bottom (12 figures): density heatmaps at different times t = 30/40/60 s (left/middle/right columns). Density is measured in pedestrians per square meter. Each row corresponds to a simulation with a given model. I: first-order Hughes' model when preferred velocity is following the shortest distance path. Pedestrians then ignore the second door. II: first-order model Hughes' model with $c(\rho) = 1/V(\rho)$. III & IV: second-order model with $C(\rho) = 1/V(\rho)$ in the Eikonal equation (10) and $P(\rho) = p_0\rho^2$ with $p_0 = 0.1$ (III) or $p_0 = 0.005$ (IV). *Figures from Twarogowska et al. (2013).*

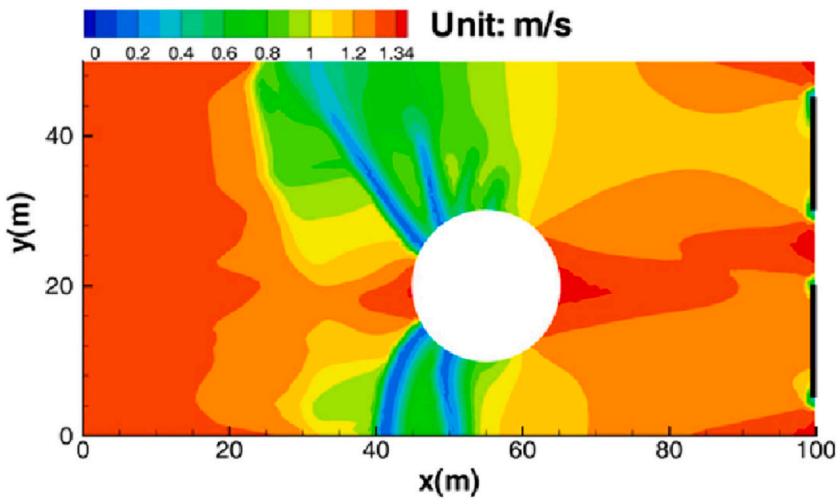

Fig. 9 Velocity field from a 2nd order model simulation for pedestrian flow around an obstacle. Some stop and go waves are visible. *From Jiang et al. (2010).*

3. Links between microscopic, mesoscopic, and macroscopic models

There are several levels at which we can model pedestrian dynamics (Duives et al., 2013). Each of these levels offers a different perspective on the problem of pedestrian dynamics. At the so-called *microscopic level*, we can consider pedestrians to be individual particles, moving in space and interacting with each other and also potentially with the environment. At the *mesoscopic level*, we "zoom out" and consider the density of particles in space at a larger scale, while allowing for a distribution of velocities at the each point in space. At the *macroscopic level*, we consider the density of particles at each point in space, but allow only one velocity at each point. In the previous section, we have focused on macroscopic models for pedestrian dynamics. In this section, we will first discuss each level and then the methods of derivation from one level to the next.

3.1 Several levels of description

3.1.1 The microscopic level

At the microscopic level, we are modelling individual interacting particles which are moving and interacting spatially. Each particle is considered to be a pedestrian, and we endow these particles with behavioral rules which dictate how they move and how they interact with others and with their environment. These models can be *deterministic* so that there is no randomness in the movement or interactions, or *stochastic* so that there is some random component to these responses. The pedestrian particles can be in *continuous space*, so that they can move anywhere on a line or surface, or they can move on a *grid* or *lattice*, so that at each timestep they can only move, for example, one spatial unit up, down, left, or right.

As a side remark, we can note that cellular Automata (CA), a popular method of modelling which is defined on a lattice, can be considered either as microscopic or mesoscopic since they sit in many ways between the two scales. With CAs, we are still able to distinguish the individuals; however, on the other hand, particles sample from a distribution of velocities when they choose to move up, down, left, or right, and the behavior on the level of individual particles can be very crude since the goal is often to have efficient simulations that will be realistic on large scales. One might therefore also reasonably identify this as a mesoscopic model. However, for the present work, we will consider CA models as a part of the microscopic scale, so that microscopic modelling includes both particle-based models

and cellular automata such as Floor Field Models (Burstedde et al., 2001; Kirchner and Schadschneider, 2002; Schadschneider et al., 2003) or exclusion processes (Schadschneider et al., 2011). We refer the reader to Chapter 7 for a deeper discussion of microscopic models.

3.1.2 The mesoscopic level

At the mescoscopic level, we can again consider families of pedestrians with different goals or preferred velocities. Each of these families is modelled by a density in space but also in velocity. Indeed, not all pedestrians will have their velocity exactly equal to the desired one or to the average velocity. Instead, pedestrians will rather have a whole distribution of velocities. Kinetic models will thus involve density distributions yielding the probability to find a pedestrian at a given location in space with a given velocity.

More precisely, the probability distribution function $f(\mathbf{x}, t, \mathbf{v}, \mathbf{g})$ gives the probability density to find a pedestrian with velocity $\mathbf{v}$ in site $\mathbf{x}$ at time t, with target $\mathbf{g}$. This last parameter $\mathbf{g}$ is new compared to the probability distribution functions used for fluids. Indeed, molecules do not have any target that will bias their motion, they just react to external forces, while pedestrians usually want to go somewhere. Pedestrians with different targets may share the same space (a street, a square, etc). They will be considered as different populations that interact on their way.

As we will detail it more in Section 3.2.3, these distributions obey Partial Differential Equations generally involving derivatives in time, space, and velocity (Dogbé, 2012; Hoogendoorn and Bovy, 2000). The pedestrians then interact with one another and the environment generally via spatial convolutions, which calculates the probable movements based on the state of the system. The canonical example of a PDE of this type is the Boltzmann Equation (Degond, 2004).

3.1.3 The macroscopic level

At the macroscopic level, we model pedestrians as a density in space. This again can be considered as the probable density of pedestrians to be found at a given spatial location, and the governing equations are again Partial Differential Equations, but now involving derivatives only in time and space. The most well-known model of this type is, for fluids, the Navier-Stokes Equation.

Though we do not detail it here, there exists also families of models based on a multiscale perspective, and we refer interested readers to (Cristiani et al., 2014; Piccoli and Tosin, 2009). We will now see how it is possible to relate the various scales through micro-macro derivations.

3.2 Methods of derivation

Because different types of information and different mathematical and statistical tools are accessible at each of the levels, it is often helpful to be able to relate the microscopic, mesoscopic, and macroscopic versions of the same model. In this subsection, we will consider different methods of derivations from one level to another, depending on the form of the microscopic model.

3.2.1 Starting from a microscopic model on a lattice

General considerations

When a microscopic model is defined on a lattice, the state of the system usually uses a discrete variable i (or two variables i,j in two dimensions), that indicates on which node (or cell) of the lattice the agent is. Typically, such a variable i ranges from 0 to L where L is the system size.

An ensemble average allows the passage from the discrete occupation numbers on the lattice to densities, or occupation probabilities. This new version of the model, sometimes called Lattice Boltzmann Equation, corresponds to the kinetic level. It is often preferable to write evolution equations for lattice models directly at the kinetic level. Indeed, instead of updating each individual - with the individual fluctuations that it implies -, we need only to consider the *averaged* modifications of each state, and these can easily be quantified using the transition rates.

Going further to mesoscopic and macroscopic scales implies that we will see the system from a largest distance, and that the discretizations will not be visible anymore. The new variable that will replace the discrete i is a continuous space variable x that we can define for example as $x = \frac{i}{L}$.

Evolution rules usually involve neighboring sites on the lattice. With the change of variable defined above, the distance between two neighboring sites i and $i+1$ is $\delta x = \frac{1}{L}$ which becomes arbitrarily small for large L. This allows us to perform Taylor expansions in the microscopic evolution equations, from which some derivatives will appear, and result into some PDEs. In two dimensions, the derivation may be more involved and as an example we refer the reader to (Burger et al., 2011) for a macroscopic derivation from the microscopic Floor Field Model of (Kirchner and Schadschneider, 2002). Another example will be given now.

An example of micro-macro derivation: The gang model

Our purpose is not only to give an example of micro-macro derivation but also to illustrate how this can be useful to gain more insight into the

dynamics of the system. We take as an example the model introduced in (Alsenafi and Barbaro, 2018), generalized in (Alsenafi and Barbaro, 2021), and analyzed in (Barbaro et al., 2021). This lattice-based model is a time-dependent version of the model for gang territorial development introduced in (Barbaro et al., 2013). In (Alsenafi and Barbaro, 2018), the authors present and study an agent-based model for territorial development, where agents from two gangs (A and B) move up, down, left, or right on a 2 dimensional lattice, putting down graffiti of their own gang's color as they move and preferentially avoiding lattice sites with the other gang's color. The movement probabilities from lattice site (i_1, j_1) are given by

$$M_A(i_1 \to i_2, j_1 \to j_2, t) := \frac{e^{-\beta \xi_B(i_2, j_2, t)}}{\sum_{(\tilde{\imath}, \tilde{J}) \sim (i_1, j_1)} e^{-\beta \xi_B(\tilde{\imath}, \tilde{J}, t)}},$$

where ξ_B denotes the density of graffiti at a site for gang B, β is parameter that symbolizes the strength of the avoidance of graffiti belonging to the other gang, and $(\tilde{\imath}, \tilde{J}) \sim (i_1, j_1)$ denotes the neighbors of site (i_1, j_1). Gang B's movement probabilities are defined similarly.

This model could be considered to be a chemo-repellent Cellular Automaton. An important feature of the model is that the agents interact only through the graffiti field and not directly, and agents are neither created nor destroyed. This means that the sites can be occupied by many agents at once, and the total number of agents of each type is conserved. In some parameter regimes, the uniform distribution of both gangs is stable, while in others, the system segregates as seen in Fig. 10. This phase transition is studied numerically at the microscopic level, and a phase transition is observed.

However, it is unclear how to determine the critical β value. The authors therefore write their model at the kinetic level, referring the density and graffiti level as ρ_k and ξ_k for $k \in \{A, B\}$, respectively, with the evolution of ρ_k given by:

$$\begin{aligned} \rho_A(i, j, t + \delta t) \;=\; & \rho_A(i, j, t) + \sum_{(\tilde{\imath}, \tilde{J}) \sim (i, j)} \rho_A(\tilde{\imath}, \tilde{J}, t) M_A(\tilde{\imath} \to i, \tilde{J} \to j, t) \\ & - \rho_A(i, j, t) \sum_{(\tilde{\imath}, \tilde{J}) \sim (i, j)} M_A(i \to \tilde{\imath}, j \to \tilde{J}, t). \end{aligned}$$

and the evolution for ξ_k given by:

$$\xi_A(i, j, t + \delta t) = \xi_A(i, j, t) - \delta t \cdot \lambda \cdot \xi_A(i, j, t) + \delta t \cdot \gamma \cdot \rho_A(i, j, t),$$

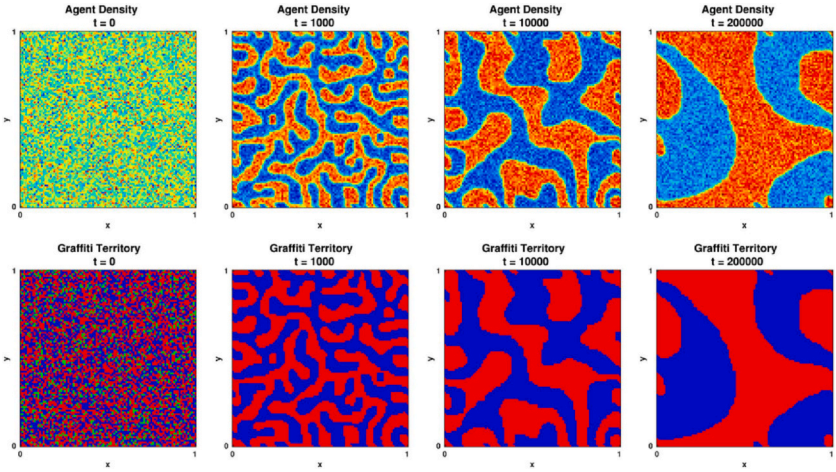

Fig. 10 Temporal evolution of the agent density lattice (top) and territory dominated by the gang's graffiti (bottom) for a segregated state. Here we have $N_A = N_B = 100,000$, with $\beta = 2 \times 10^{-5}$, $\lambda = \gamma = 0.5$, $\delta t = 1$ and the lattice size is 100×100. It is clearly seen that both the agents and the territory dominated by graffiti segregate over time for these parameters. *Figure and caption are reproduced from Alsenafi and Barbaro (2018).*

Here, λ is a decay rate for the graffiti and γ is its deposition rate by the members of the gang. From this kinetic description, and introducing the continuous variables $x = \frac{i}{L}$ and $y = \frac{j}{L}$, the authors then use Taylor expansion and the discrete Laplacian to formally derive a macroscopic model consisting of four coupled PDEs:

$$\begin{cases} \frac{\partial \xi_A}{\partial t}(x, y, t) = \gamma \rho_A(x, y, t) - \lambda \xi_A(x, y, t) \\ \frac{\partial \xi_B}{\partial t}(x, y, t) = \gamma \rho_B(x, y, t) - \lambda \xi_B(x, y, t) \\ \frac{\partial \rho_A}{\partial t}(x, y, t) = \frac{D}{4} \nabla \cdot [\nabla \rho_A(x, y, t) + 2\beta (\rho_A(x, y, t) \nabla \xi_B(x, y, t))] \\ \frac{\partial \rho_B}{\partial t}(x, y, t) = \frac{D}{4} \nabla \cdot [\nabla \rho_B(x, y, t) + 2\beta (\rho_B(x, y, t) \nabla \xi_A(x, y, t))]. \end{cases}$$

We refer to (Alsenafi and Barbaro, 2018) for the details.

The authors then are able to analyze the model at the macroscopic level using a standard linear stability analysis to identify where the uniform equilibrium loses stability, at

$$\beta_c = \frac{1}{2\left(\frac{\gamma}{\lambda}\right)\sqrt{\overline{\rho}_A \overline{\rho}_B}},$$

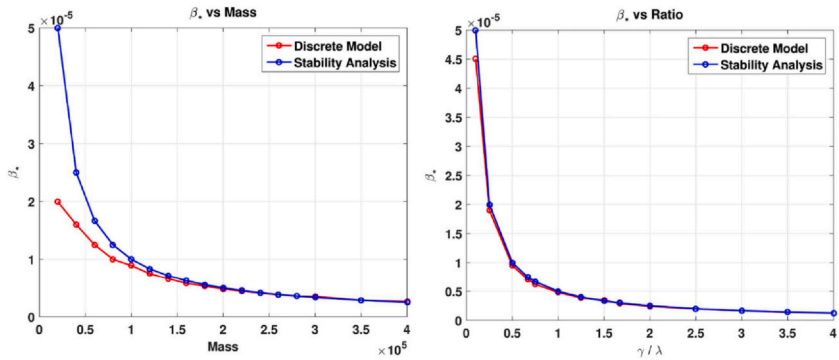

Fig. 11 On the Left: critical β against the system mass. Here we have that $\lambda = \gamma = 0.5$, and for the discrete model we have that $\delta t = 1$ and the lattice size is 50×50. The red and blue curves represent the discrete model and the linearized PDE system respectively. On the right: critical β against the ratio $\frac{\lambda}{\gamma}$. Here we have $N_A = N_B = 100,000$, and for the discrete model we have that $\delta t = 1$ and the lattice size is 50×50. The red and blue curves represent the discrete model and the linearized PDE system respectively. *(For interpretation of the references to color in this figure legend, the reader is referred to the web version of this article.) Figure and caption are reproduced from Alsenafi and Barbaro (2018).*

where $\overline{\rho}_A$ and $\overline{\rho}_B$ denote the average density of gangs A and B over the lattice, respectively. Fig. 11 shows the numerical results of the phase transition plotted on the same axes as the β_c resulting from the stability analysis, and it can clearly seen that the critical parameters from the discrete model agree with the one found by analyzing the macroscopic version of the model, as long as the system mass, i.e. the number of agents, is sufficiently high (this is to be expected, since the derivation is formal and therefore assumes sufficient smoothness of the quantities of interest, so the derivation cannot be expected to hold if the density is not sufficiently smoothly distributed).

The example from (Alsenafi and Barbaro, 2018) serves to demonstrate the usefulness of deriving a macroscopic description of the microscopic particle model. Indeed for many models, more mathematical machinery is available to analyze a macroscopic description, and this can then offer insight which is not accessible at the microscopic level.

3.2.2 Starting from an off-lattice microscopic model in one dimension

We now consider a microscopic model in continuous space. A first approach coming from car traffic (Aw et al., 2002; Tordeux et al., 2018) assumes that we can order the pedestrians as leaders and followers. This will occur in

particular in one dimensional lines, as for example in a corridor. Pedestrians are numbered and we use here the convention that pedestrian i is following pedestrian $i-1$. The discrete variable i is now a Lagrangian variable, attached to the agent or particle itself. Ped-following or Follow-the-Leader models (Lemercier et al., 2012; Rio et al., 2014; Fehrenbach et al., 2015; Tordeux et al., 2017) typically express the velocity or acceleration of the follower i as a function of the distance, speed difference, etc, with the leader $i-1$.

With such models, two steps are necessary in order to derive a macroscopic model. We must not only go from a discrete to a continuous description, but also from a Lagrangian (we follow the agents) to an Eulerian (we observe the flow at a fixed location) description. The first step is realized by defining a new Lagrangian variable $y = i \times \delta_0$ where δ_0 can be for example the minimum distance between two pedestrians. When we look at the system from a distance, taking formally in the limit $\delta_0 \to 0$, y becomes a continuous variable. We have in particular that $dy = di \times \delta_0$. The second step is to relate the infinitesimal variation of the Lagrangian variable dy to the infinitesimal variation dx of the Eulerian variable, at fixed time. The link between the two variables is illustrated in Fig. 12. One key point is to realize that though dx is infinitesimal, it is still large compared to the distance between vehicles. Besides, the micro-macro derivation is done under the hypothesis that everything varies slowly in space. Following this assumption, we have that interspaces are constant within the dx and equal in particular to Δx_i. As a result, we can write that

$$\frac{dy}{\delta_0} = di = -\frac{dx}{\Delta x_i}. \tag{16}$$

where the ratio $\frac{dx}{\Delta x_i}$ is the number of pedestrians located within dx, and thus tells how much i varies within dx. The minus sign comes from the convention that i is decreasing for increasing x.

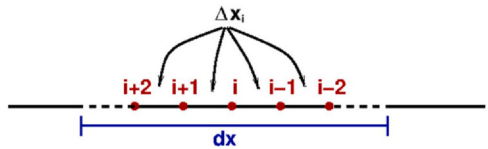

Fig. 12 Schematic representation of the link between the discrete Lagrangian variable i and the continuous Eulerian variable x. Agents (red dots) are numbered so that pedestrian i is following pedestrian $i-1$. On a scale dx, interpersonal distances are the same for all successive pairs of leader-follower (assumption of slow spatial variations) and we take all of them equal to Δx_i.

A microscopic density can be defined from the individual interspace, that will allow to make the link with the macroscopic Eulerian density:

$$\frac{\delta_0}{\Delta x_i} = \rho_i(t) = \rho(X_i(t),\, t) \tag{17}$$

Here the first ρ_i is still the Lagrangian density function, while the second one is Eulerian. The coefficient δ_0 can be seen as a normalization of the density such that, for example, $\rho_{max} = 1$.

From relations (16)–(17), we get the variation of x when y varies at fixed time, ie the partial derivative

$$\frac{\partial x}{\partial y} = -\frac{1}{\rho} \tag{18}$$

For more obvious reasons, the variation of x in time for fixed y - ie for fixed pedestrian number - is the velocity:

$$\frac{\partial x}{\partial t} = v \tag{19}$$

Once such relations are obtained, it is possible though somewhat lengthy to go from the Lagrangian time derivatives and neighbor-to-neighbor variations in the microscopic ped-following model to the Eulerian PDEs. We refer the interested reader to (Aw et al., 2002; Tordeux et al., 2018; Zhang, 2003; Burger et al., 2019) for the full calculation in the frame of various car or ped-following models.

3.2.3 Starting from an off-lattice microscopic model in two dimensions

The situation is different when pedestrians evolve in 2 dimensions. It is then not possible anymore to number them in terms of leader/follower, and the derivation of the kinetic equations is more tricky.

Ideally, one would like to be able to perform an ensemble average on the microscopic dynamics, to deduce a partial differential equation for the evolution of the distribution function for the probability density $f(\mathbf{x}, t, \mathbf{v}, \mathbf{g})$ to find a pedestrian with velocity $\mathbf{v}$ in site $\mathbf{x}$ at time t, with target $\mathbf{g}$. Though the ensemble average allowing to find the kinetic equation is in principle similar to the derivation of the Boltzmann equation from molecular dynamics, pedestrian microscopic models are in general too complicated for a rigorous derivation.

One possibility is to redefine the microscopic dynamics to simplify it while keeping the main ingredients. For example we can assume that

pedestrians only modify the direction of their velocity, while keeping a constant speed modulus - an assumption that will restrict the use of the model to low densities (Degond et al., 2013b). Another possibility is to replace discontinuous changes of the pedestrian velocity by continuous time evolutions. If, moreover, the rate of change of the velocity can be expressed for example as the gradient of some function, it will be easier to find an equivalent formulation at the kinetic level (Degond et al., 2013b, 2013a).

A difficulty that is often encountered is that many models implement a reaction to the most threatening collision. The quantifier of the collision threat could be, for example, the time until predicted collision. Then the model requires finding the maximum or minimum of such quantified collision threats. This max/min operation is easy to perform when a pedestrian undergoes only a finite number of interactions. However, in contrast, when considering continuous probability distributions, there is always a more threatening collision that could occur, maybe with very low probability but not strictly impossible. A similar problem is met when the pedestrian dynamics is determined from the minimization of some cost function. One way to deal with this problem is to replace the max/min function in the microscopic agent based model by some average, or median, of some distribution based term in the kinetic model (Degond et al., 2013b, 2013a).

The general form of a kinetic equation for probability density function f will be

$$\partial_t f + \mathbf{v}\cdot\nabla_{\mathbf{x}} f + Sf = Lf \tag{20}$$

where Sf contains all the interactions that modify the distribution, in general with terms involving derivatives in $\mathbf{v}$, and Lf is some diffusive term resulting from stochastic forces. Indeed, some noise is often added to the microscopic dynamics, to account for a wider variety of behavior. It produces diffusion at the mesoscopic level, and at the macroscopic level, it will allow to have smoother closures (Degond et al., 2013a).

Once the kinetic equation is found, we would like to derive a macroscopic model for the density $\rho(\mathbf{x}, t, \mathbf{g})$ and the velocity $U(\mathbf{x}, t, \mathbf{g})$, which are related to the distributions through

$$\rho(\mathbf{x}, t, \mathbf{g}) = \int f(\mathbf{x}, t, \mathbf{v}, \mathbf{g})\, d\mathbf{v} \tag{21}$$

$$\rho(\mathbf{x}, t, \mathbf{g})\, U(\mathbf{x}, t, \mathbf{g}) = \int f(\mathbf{x}, t, \mathbf{v}, \mathbf{g})\, \mathbf{v} d\mathbf{v}. \tag{22}$$

Both integrals above are taken over all possible values of the velocity, allowing us to extract a classical density field ρ in (21) and an average macroscopic velocity field U in (22). The moment method consists in multiplying the kinetic equation by polynomials involving increasing powers of $\mathbf{v}$ before integrating (Dogbé, 2012). Unfortunately, the resulting set of equations is in general not closed, and one need to supplement it by some closure relation.

To be specific, we see from (21)–(22) that the direct integration of (20) will provide an equation for ρ that involves ρU. Multiplying (20) by v before integrating will provide an equation for ρU that involves still higher moments of the velocity. We could find an equation for this higher moment, but it will always involve a moment of even higher degree. This is why it is necessary to make an assumption to close this hierarchy of equations.

Such closure relation can be provided by an ansatz that expresses the distributions f as a function of the macroscopic variables ρ and U. Note however that in general one cannot justify the choice made for this ansatz, in contrast with the case of fluids (Degond et al., 2013a).

One of the easiest one is the *mono-kinetic* closure, which assumes that all particles of the same family have their velocity exactly equal to the average macroscopic velocity. In mathematical terms, this is expressed by a factor $\delta_{U(\mathbf{x},\ t,\ \mathbf{g})}(v)$ in the distribution (Salam et al., 2021; Degond et al., 2013a, 2013b). But other choises can be made, that allow for some dispersion of the velocity around the average value (Degond, 2004; Degond et al., 2013a, 2013b).

While many derivations of continuum models from particle dynamics are formal, i.e. relying on assumptions about the smoothness of the solution, etc., there are also some relatively recent results rigorously deriving kinetic descriptions of particle models. In particular, we refer the interested reader to (Canizo et al., 2011) for rigorous derivation from (some) particle systems to kinetic equations.

4. Incorporating specifics of crowd behavior

Though the models we have described so far are able to reproduce some of the features of crowds dynamics, they are far from capturing the whole complexity of these. Various attempts have been made in the past decades to include more of the physics of crowds in the models. Here we

present some directions of research that allow to take into account the non-locality of interactions, the heterogeneity of crowds, and their ability to anticipate.

4.1 Taking granularity into account

In order to illustrate the different behavior of micro and macroscopic models, let us compare both as done in (Maury et al., 2011) for an evacuation problem (Fig. 13). If we consider a microscopic model (Left), and its macroscopic counterpart (Right), we find first a very similar behavior: see in Fig. 13-Top) the same low density regions behind obstacles and high density accumulations in front of bottlenecks (Maury et al., 2011).

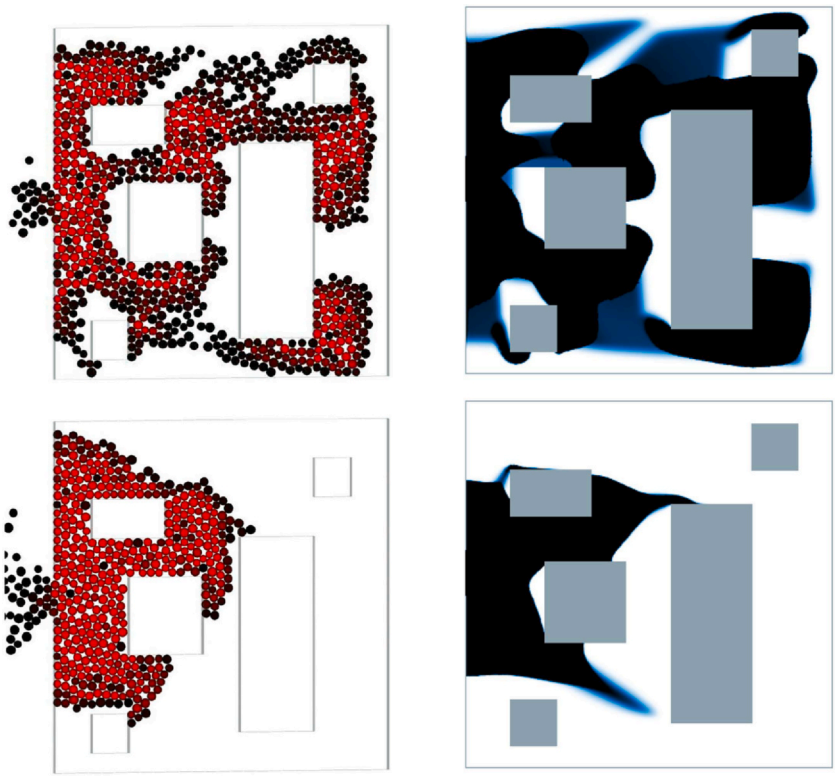

Fig. 13 Evacuation by a door located on the left of an area containing several obstacles. The crowd is simulated either by a microscopic (left) or macroscopic (right) model, and is shown at an earlier (top) or later (bottom) stage. *From Maury et al. (2011).*

However, looking at longer time evolution reveals a striking difference (see Fig. 13-Bottom): evacuation is more rapid with the macroscopic model than with the microscopic one.

Indeed, granularity plays a role at bottlenecks. The transient formation of arches slows down the exit of pedestrians, a feature which is correctly captured with the microscopic model, but is ignored by the macroscopic description. In a macroscopic model, the crowd is considered as a fluid, that would in particular be able to flow through a narrow exit of a few centimeters - a feature clearly unrealistic. The lack of granularity in macroscopic models gave raise to several approaches that aim to correct for this shortcoming.

4.1.1 Non-local macroscopic models

Granularity gives raise to non-local effects at exits. One way to include non-locality in macroscopic models is to estimate the flux or velocity not from a purely local density, but from a non-local density averaged on the surroundings of x. Namely, the velocity would be combined with a convolution kernel w_η, which allows making an average with different weights depending on the distance (Colombo et al., 2011).

An example coming from car traffic modelling (Blandin and Goatin, 2016) would be

$$\partial_t \rho(t, x) + \partial_x \left[\rho(t, x) V\left(\int_x^{x+\eta} \rho(t, y) w_\eta(y - x)\, dy \right) \right] = 0$$

The convolution kernel w_η must be a non-increasing function such that $\int_0^\eta w_\eta(x)\, dx = 1$. We can take for example, $w_\eta(x) \equiv 1/\eta$ or $w_\eta(x) = 2(1 - x/\eta)/\eta)$, where η is a positive parameter that can be freely chosen. This downstream convolution product models the fact that agents react to what happens downstream. For crowds, kernels in two dimensions should be used and it is possible to choose anisotropic kernels in order to account for a finite vision field (Bürger et al., 2020; Goatin et al., 2025; Cristiani et al., 2015).

For pedestrians, non-locality can also be included in the definition of the direction of the desired velocity (Colombo and Lécureux-Mercier, 2012; Colombo et al., 2012; Campos et al., 2021; Bürger et al., 2020). Typically, the direction of the preferred velocity would be written as

$$\nu(\mathbf{x}, t) = \mu(\mathbf{x}) + \mathcal{I}[\rho(t)](\mathbf{x}) \tag{23}$$

where μ would be a fixed preferred velocity field coming from an Eikonal equation - in general μ would follow the shortest paths -, and $\mathcal{I}$ would be a functional of the density field $\rho(t)$ that depends on the gradient of the density convoluted with an averaging kernel, so that it is non local. It makes pedestrians able to turn in order to avoid regions of increasing density. This provides an easy way to implement walls. If walls are given a high density, pedestrians will avoid them.

The model can be extended to several species of pedestrians by associating an equation to each species. When extended to bi-directional flows, such non-local model can reproduce lane formation (Colombo and Lécureux-Mercier, 2012; Goatin et al., 2024), a feature which is not possible with purely local models. Similarly, non-local models can reproduce the stripe formation at the intersection of perpendicular flows (Goatin et al., 2024).

Another advantage of non-local models is that well-posedness is obtained more easily than for local models, for which hyperbolicity is more easily lost. Micro-macro derivations can also be performed for non-local models, see (Chiarello et al., 2020) for an example.

4.1.2 Local and non-local point constraints

Another way to account for granularity is to model directly the flux limitation it induces at bottlenecks. This is useful mainly in one dimensional systems for which flux limitation does not come from the geometry. Bottlenecks can be considered as objects that impose locally a constraint on the flux (Andreianov et al., 2018; Chalons et al., 2013)

$$f(\mathbf{x}_i, t) \leq Q_i \tag{24}$$

where Q_i is the maximal value of the flux at the specific location $\mathbf{x}_i$ of a bottleneck.

The constraint is local if Q_i depends only on the local density $\rho(\mathbf{x}_i)$, and non-local if Q_i is a non-local expression of the density (Santo et al., 2019). Such constraints can be imposed in the frame of a first-order model (Santo et al., 2019; Colombo et al., 2010) as well as second-order (Andreianov et al., 2016, 2021).

4.2 Taking heterogeneity into account

It is also possible to consider more than one type of pedestrian, for example multiple groups each with a preferred destination or velocity (Hartmann and von Sivers, 2013). This can account for differences such as a variety of ages, heights, or levels of mobility, traveling with luggage, family groups traveling together, or as discussed previously, multiple gangs (Alsenafi and

Barbaro, 2018). In the context of disease propagation, it is necessary to distinguish infected people from others (Salam et al., 2021).

Though there is still a debate about the role emotions can play in evacuation processes (Lügering et al., 2023), several models have also considered the emotions of the pedestrians. For example, (Burstedde et al., 2001) introduces two moods into their Floor Field model, with differing movement dynamics for each: Happy pedestrians move in their preferred direction while unhappy pedestrians undergo more random movement. There are update rules for switching pedestrians between happy and unhappy moods.

Including an emotional variable which undergoes contagion is another type of model for heterogeneous crowds. The authors in (Bosse et al., 2011) introduce an agent-based (microscopic) model for fearful crowds which they call the ASCRIBE model. Each agent is endowed with an emotion level and the emotion levels of the agents change via interactions with nearby agents. The authors apply this ASCRIBE model to video of a stressful situation in a crowd in Amsterdam. The ASCRIBE model is further studied in (Tsai et al., 2011), where it is found to compare favorably in two case studies to another agent-based contagion model in the literature, referred to as the ESCAPES model (Durupınar, 2010). In (Bertozzi et al., 2015), the authors again begin with the ASCRIBE model, but then derive mesoscopic and macroscopic descriptions which describe the evolution of the densities including this extra emotional component. The emotional variable dictates the speed of the particles. Numerical techniques for this mesoscopic model were developed in (Wang et al., 2017).

It is important to note here that the mesoscopic description is able to capture a distribution of emotion levels or velocities at a single point in space, and thus describe a heterogeneous population. When it is important that there is a mixture of fear levels - or actually a mixture of any type of characteristics - this distribution cannot be replaced by an average value. Thus we cannot go to macroscopic level, and we need to keep the microscopic or kinetic description in the region of mixture. These mesoscopic descriptions are therefore one way to include heterogeneity at the level of a continuum model.

4.3 Mean field game models: Taking anticipation into account

When pedestrians compete for space (for example in a congested situation), they develop some strategy, meaning that they choose a trajectory in order to optimize their exit time, comfort, etc. They can do this based on the

current state of the system (optimal control) or they can anticipate that others will themselves try to anticipate and optimize (game theory). To this end, before describing mean field games, we will as a first step introduce optimal control ideas.

4.3.1 Cost and optimal control

One way to model pedestrian dynamics is to assume that they try to minimize some cost. A first step is to determine which cost is minimized (Arechavaleta et al., 2008; Chitour et al., 2012). Usually one considers that the cost is proportional to the distance to walk, but other quantities like the jerk can also be taken into account. One may give different weights to longitudinal acceleration and side-stepping (Hoogendoorn and Bovy, 2003), or associate a cost for departing from a physiologically optimal speed (Guy et al., 2012). Crowds can avoid to form high density regions, or on the contrary, if the crowd wants to stay in a group, they may minimize the space occupied by the crowd (Herzog et al., 2023).

Once the cost is defined, its minimization will determine, or at least influence, the pedestrians dynamics. Cost minimization can be used in the frame of microscopic models (Hoogendoorn and Bovy, 2003, 2004) or, at an urban scale, of networks (Alisoltani et al., 2024), though here we are interested in its use for macroscopic models. Actually we saw already such an example, given by the Eikonal equation (10) of Section 2.1.4 (Hughes model).

When the cost depends only on static quantities, for example when it amounts at minimizing the distance to the exit, it is sufficient to solve once the Eikonal equation at the beginning of the simulation. However when the cost depends for example on the density, the minimization must be performed at regular intervals to account for the evolution of the surroundings, including the presence of jammed areas (Hoogendoorn and Bovy, 2004; Hoogendoorn et al., 2015). In particular in Hughes model, only the current state of the density field is taken into account. The Eikonal equation (10) is a kind of static Hamilton-Jacobi equation, for which many numerical methods have been developped (Twarogowska et al., 2013).

4.3.2 Mean-field games

When several pedestrians want to perform a similar task, such as exiting through a given exit, they may be in competition for space. Indeed, two persons cannot be at the same place at the same time. Games are appropriate to describe this competitive situation. They assume that pedestrians can anticipate others' behavior, and optimize their own strategy (namely

choosing their walking behavior) in order to minimize their own cost. A Nash equilibrium is expected to be reached, in which nobody has some interest to change its strategy. However, when many pedestrians are involved in the game, it would be too costly to solve the full game involving all the individuals.

Mean field games (MFG) were proposed by Lasry and Lions (2006) and Huang et al. (2006) to circumvent this difficulty. The idea is that, instead of having to consider all the individual interactions, each pedestrian reacts to the *average* density that can be expected in all future locations. MFGs can a priori be written for very general forms of the cost. They were used in particular for dynamic traffic assignment in transportation networks (Ameli et al., 2022; Khoshyaran and Lebacque, 2024). The special case where the velocity - namely the strategy of the pedestrian - appears in the cost as a quadratic term (Ullmo et al., 2019; Benamou et al., 2017) turned out to be well suited for pedestrians (Dogbé, 2011; Lachapelle and Wolfram, 2011; Burger et al., 2014).

Typically, a quadratic MFG gives the coupled evolution of the pedestrians density ρ and of the so-called value function u which is the value of the individual cost after optimization

$$u(\mathbf{x}, t) = \inf_{\mathbf{a}} \mathbb{E}\left\{\int_t^T \left[\frac{\mu}{2}\mathbf{v}^2 - V[\rho]\right] d\tau + c_T(\mathbf{x}_T)\right\}. \tag{25}$$

The quadratic MFG can be thus expressed as the following coupled evolution equations

$$\begin{cases} \partial_t \rho(\mathbf{x}, t) = \frac{1}{\mu}\nabla\cdot[\rho(\mathbf{x}, t)\nabla u(\mathbf{x}, t)] + \frac{\sigma^2}{2}\Delta\rho(\mathbf{x}, t) \\ \partial_t u(\mathbf{x}, t) = \frac{1}{2\mu}[\nabla u(\mathbf{x}, t)]^2 - \frac{\sigma^2}{2}\Delta u(\mathbf{x}, t) + V[\rho](\mathbf{x}, t) \end{cases} \tag{26}$$

The first equation of (26) expresses once more mass conservation, but now with a diffusion term that comes from microscopic noise. The velocity in the first term of the right-hand side has been replaced by its value resulting from the optimization process, namely $-\frac{1}{\mu}\nabla u$. The second equation is derived using the theory of dynamical programming and we will not give here the details of this derivation. It is based on the idea that in order to optimize from a current time t, you do not need to take into account the past but only the future.

The boundary conditions necessary to solve the equations (26) involve the terminal cost $c_T(\mathbf{x}_T)$ and the initial density field

$$\begin{cases} u(\mathbf{x},\, t = T) = c_T(\mathbf{x}) \\ \rho(\mathbf{x},\, t = 0) = \rho_0(\mathbf{x}) \end{cases} \tag{27}$$

It can be noticed, in particular through the boundary conditions and the sign in front of the Laplacian terms in (26), that the equation for ρ is forward in time, but the equation for u – the so-called Hamilton-Jacobi-Bellman equation – is backward in time. This forward-backward structure makes it difficult to solve even numerically, and it can be sometimes useful to exploit the mapping that exists between system (26) and a system of two coupled Non-Linear Schrödinger equations (Ullmo et al., 2019; Bonnemain, 2020; Bonnemain et al., 2020).

MFGs are able to reproduce typical behavior of crowds as lane formation in bi-directional flows (Lachapelle and Wolfram, 2011), as most models can do. More interestingly, MFGs were the first method able to reproduce some experimental results, namely the deformation of a crowd around a cylindrical intruder (Nicolas et al., 2019; Appert-Rolland et al., 2020), that require long range anticipation. Indeed in most models, pedestrians either do not anticipate, or only up to the next collision. In MFGs, the cost implies that pedestrians have a full knowledge of the future up to time T, which can be made as large as we want - up to infinite if needed. In the case of the aforementioned experiment, it can be assumed that pedestrians have a sufficient experience of obstacle avoidance to be able to anticipate not only their own behavior but also the one of others. As a result, as illustrated in Fig. 14, the MFG is able to reproduce the density and velocity patterns around the cylinder, while other methods fail (Bonnemain et al., 2023; Butano et al., 2024b).

Full anticipation may be a too strong assumption (Cristiani et al., 2015, 2023) and it is possible to add a discount factor $e^{\gamma(t-\tau)}$ in the cost of Eq. (25) to account for the fact that pedestrians have a better knowledge of what happens closer in time (Hoogendoorn and Bovy, 2003; Dogbé, 2011; Lachapelle and Wolfram, 2011; Butano et al., 2024a). This allows to explain why the experimental results can be different when pedestrians face or present their back to an incoming obstacle (Butano et al., 2024a). Instead of assuming that agents instantaneously choose the Nash equilibrium, it is also possible to assume that agents only tend towards this goal (Degond et al., 2014).

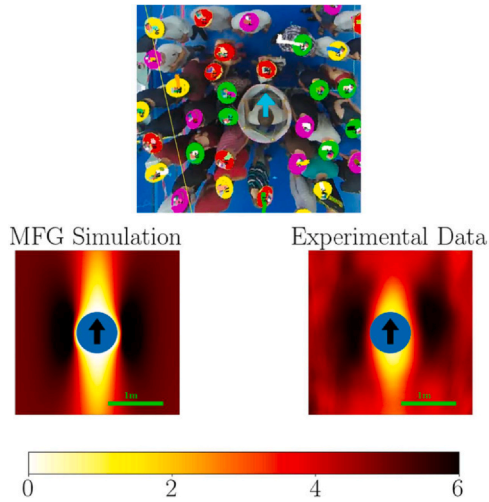

Fig. 14 Top: Experimental setup for the crossing of a crowd by a cylindrical intruder. Bottom: comparison of the density field (in ped/m^2) obtained by MFG simulation (left) and reconstructed from the experimental data (right). *Top: From Nicolas et al. (2019), Bottom: From Butano et al. (2024a).*

5. Numerical simulation of macroscopic models

In this section, we focus on numerically solving macroscopic pedestrian models, which is an inherently Eulerian problem. We will distinguish two main approaches. In the first approach, we keep the Eulerian variables of density and velocity but discretize the spatial and time domains. The second approach uses virtual particles, such that the evolution of these particles dictates the numerical solution of the macroscopic equation. We will describe several approaches of each type within the pedestrian dynamics community, and discuss the challenges associated with each framework.

5.1 Grid-based Eulerian methods

In this framework, the macroscopic models are generally solved using canonical methods for solving hyperbolic PDEs: Finite Difference Methods (FDMs), Finite Element Methods (FEMs), and Finite Volume Methods (FVMs). With these methods, the challenges are the same as for solving many problems in PDE: gradients can become very steep, requiring either a very fine grid or a shock description; numerical viscosity can artificially smooth shocks for some methods, while oscillations around shocks can be a

problem for others (LeVeque, 1992), and specific methods have been developed to handle shocks. Instabilities can also occur near the maximal density limit, as in (Appert-Rolland et al., 2011). Additionally, loss of mass induced in numerical methods that do not explicitly enforce mass conservation can be of concern, forcing a fine grid in order to approximate the conservation of mass necessary for these problems. Still, many excellent numerical schemes for macroscopic pedestrian flows are non-conservative; for a more thorough discussion, the reader is referred to (Chalons, 2007) and (Chalons et al., 2013).

The most straightforward way to solve the macroscopic models is with Finite Difference Methods. In these methods, both time and space are discretized, and derivatives are approximated using difference equations. In one dimension, ρ_x and ρ_t could simply be approximated by

$$\rho_x(x_i, t_j) \approx \frac{\rho(x_{i+1}, t_j) - \rho(x_{i-1}, t_j)}{2\Delta x} \tag{28}$$

and

$$\rho_t(x_i, t_j) \approx \frac{\rho(x_i, t_{j+1}) - \rho(x_i, t_j)}{\Delta t} \tag{29}$$

for time step Δt and spatial step Δx. In these methods, more accurate results are attained by refining the grid, enforcing a smaller spatial discritization and smaller timesteps. However, this must be done with care, since violations of the Courant-Friedrichs-Lewy (CFL) condition can lead to loss of stability for the numerical method, yielding erroneous numerical solutions (Courant et al., 1928). In explicit time and space discretization schemes, the CFL condition provides upper bound for the ratio of the spatial step Δx multiplied by the velocity and the time step Δt, ensuring that no mass can artificially "skip over" a cell of the spatial grid. This condition is necessary (but not sufficient) to ensure stability of the method. For hyperbolic PDEs in one dimension, this constraint takes the form:

$$\frac{|v|\Delta t}{\Delta x} \leq C_{\max}.$$

In two dimensions, the CFL condition may be expressed as (Toro, 2009)

$$\Delta t\left(\frac{\max_i |v_i|}{\Delta x_i}\right) \leq C_{\max},$$

where $|v_i|$ is the magnitude of the velocity in the ith direction, but sometimes other expressions are used, for example using $\Sigma_i|v_i|$ in place of

the max. The CFL condition becomes a problem in areas where the velocity becomes extremely large, since the time step must be made extremely small in order to compensate. Additionally, first-order finite difference schemes tend to "smear out" shocks, introducing artificial diffusion, while second-order methods often produce oscillations on one or both sides of a shock (LeVeque, 2002).

That oscillations tend to occur in places where the derivatives become steep is particularly problematic in pedestrian dynamics, since the occurrence of shocks is a prominent feature in these models. These oscillations can be addressed by semi-discrete schemes, which first discretize the problem in space. Time is then still continuous, and the problem reduces to a system of ODE problems which can be solved using any standard method. This approach is also called the method of lines (LeVeque, 2002) and can be used to develop highly accurate numerical schemes which avoid oscillations around shocks. In particular, Essentially Non Oscillatory (ENO) and Weighted Essentially Non-Oscillatory (WENO) schemes are of this type (Harten et al., 1997). In the pedestrian literature, for example 3rd (Goatin et al., 2024, 2025) or 5th (Bürger et al., 2020) order WENO schemes were used to simulate non-local models, as well as the Hughes model (Huang et al., 2009), allowing for good accuracy in smooth regions while being able to handle the discontinuities without oscillations.

Finite Volume Methods again discretize space and time, focusing on the influx and outflux of mass through each surface of a spatial cell. These methods are conservative, since mass is transferred directly between adjacent cells. FVMs solve a collection of Riemann problems, addressing the need to admit shock solutions (LeVeque, 2002), in particular through the so-called Godunov schemes (Toro, 2009). Because pedestrian models are known to produce non-smooth solutions (i.e. ones with blowup in the density or the derivatives of the density, for example in the case of shocks), Finite Volume Methods are often preferred (Dogbé, 2008).

Another numerical approach is to use Finite Element Methods to solve the macroscopic model. In broad strokes, FEM divides the spatial domain into irregular geometrical cells (the elements) that can locally adapt to the boundaries. On each element, an ODE can be solved in place of the PDE. It is the relationship among the elements that takes care of the spatial derivatives. Eventually the full solution is constructed by weighting the solution on each element in order to minimize some global error. One significant advantage of the FEM is that boundaries and complicated geometries are easy to address, since they can be naturally included when determining the

elements. Examples of FEMs used to numerically solve pedestrian models include the discontinuous Galerkin method which makes use of discontinuous piecewise polynomial functions (Xia et al., 2009).

Another technique called a splitting scheme can be employed in macroscopic pedestrian models that take the following form

$$\frac{\partial \rho}{\partial t} + \nabla \cdot (F,\, G) = S.$$

With this method, the problem is split into two separate problems, solving

$$\frac{\partial \rho}{\partial t} = S,$$

for part of each time step, while solving

$$\frac{\partial \rho}{\partial t} + \nabla \cdot (F,\, G) = 0,$$

on the rest of the time step. Each of the two problems is solved using the most appropriate method for problems of that type (Jiang et al., 2010), leading to an accurate and more efficient numerical method.

Multiscale Eulerian approaches can also be employed in pedestrian models. For example, the paper by Wang, Short, and Bertozzi on numerically solving the contagion model (Wang et al., 2017) has several approaches for solving the model derived in (Bertozzi et al., 2015), which exhibits shocks. These include multiscale modelling by using the macroscopic formulation in regions where characteristics do not cross, while the kinetic formulation is used in areas where the characteristics are crossing. Another approach proposed in (Wang et al., 2017) is to use a level set formulation which allows for a distribution of velocities throughout the whole domain, similar to the kinetic formulation.

5.2 Particle methods

Particle methods are a different numerical framework which is also widely used in the pedestrian dynamics literature, see (Salam et al., 2021) for an example. In particle method approaches, the numerical solution of the macroscopic equation is a linear combination of Dirac delta functions (one may consider these to be weighted particles) distributed throughout the spatial domain. The weights and the positions of the particles evolve according to the macroscopic equation. An overview of deterministic particle methods can be found in (Chertock, 2017). Particle method approaches are useful because they often avoid the problem of numerical

diffusion. This is a very useful characteristic when working with macroscopic pedestrian models, since these can exhibit shocks and other diffusion-sensitive features.

One class of methods, called meshfree Generalized Finite Difference Methods, uses these particles as a an alternative to the regular grid used in Finite Difference Methods above. In this cases, the particles are stationary and are generated in the beginning of a simulation. They are irregularly spaced and used as stationary set of points at which to solve the macroscopic equation, in the spirit of a random irregular mesh. The main challenge here is determining initially the distribution of particles, called a point cloud. The interested reader is directed to (Suchde et al., 2023) for an overview on how to generate such point clouds. In (Maity et al., 2024), the authors numerically simulate several well-studied macroscopic models for pedestrian dynamics using such a meshfree Generalized Finite Difference Method with a Godunov-type discretization. They find that this numerical method captures the particular characteristics of each model.

As an alternative to the Eulerian framework with density and velocity moving on a grid or set of stationary particles, the evolution of fluid equations can also follow packets of fluid as they move through space. This is the Lagrangian Framework. Particle methods such as Smoothed-Particle Hydrodynamics (SPH) use this Lagrangian framework to numerically solve macroscopic equations. In SPH, the particles move through space with the velocity dictated by the macroscopic equation and interact with one another through an interaction kernel of radius h. This interaction determines the evolution of the physical quantities associated with each of the particles (primarily mass). It is possible to change h according to how dense the particles are in space. SPH is employed in solving macroscopic pedestrian models, for example in (Yuan et al., 2020). In (Toll et al., 2021), the authors use a hybrid Lagrangian approach by blending an agent-based model for pedestrian dynamics with a SPH method in high density scenarios.

Lagragian particle methods are also used on pedestrian models at both the microscopic and macroscopic scales in (Etikyala et al., 2014), ranging from a microscopic interacting particle model paired with the Eikonal equation to a model consisting of a nonlocal continuum equation. Other numerical methods for macroscopic pedestrian dynamics use semi-Lagrangian schemes, where the Lagrangian framework is combined with the Eulerian one, see, for example, (Carlini et al., 2017) and (Falcone and Ferretti, 2014).

As the reader can deduce, both Eulerian and particle-based numerical methods for macroscopic models of pedestrian dynamics are well-grounded and important to the field. Eulerian approaches face challenges such as numerical viscosity, oscillations, and loss of mass. In Eulerian approaches, these challenges are answered with finer meshes and therefore smaller timesteps (according to the CFL condition, as described above). It is also important to bear in mind that Eulerian simulations of macroscopic models can have many challenges with stability and well-posedness, so it is also often helpful to move to a particle method for simulations. Particle methods avoid artificial viscosity, often capturing shocks well, but encountering problems with particle distribution and computational complexity. In particle-based methods, more accuracy often requires more particles and, in some cases, redistribution of these particles, which can lead to the number of particles becoming prohibitively expensive.

6. Final discussion

Macroscopic models originated by expressing conservation of mass in a similar way to traffic models. With new features such as nonlocality and other variations like heterogeneous populations (accessible through multiple different classes of pedestrians, for example, or through mesoscopic descriptions), macroscopic models have recently begun to better approximate the specifics of pedestrian dynamics.

While microscopic pedestrian models can closely approximate the dynamics of individual pedestrians, macroscopic models can be useful in situations with a high density of pedestrians for understanding the macroscopic or system-level behavior of these large groups. Indeed, macroscopic modelling of pedestrians allows for insight into the overall group dynamics, such as the density waves (Bain and Bartolo, 2019; Gu et al., 2025), phase separation (Alsenafi and Barbaro, 2018), or pattern formation (Hoogendoorn et al., 2014; Cividini et al., 2013). These types of behaviors are most easily understood at the macroscopic level.

When working with macroscopic models, it is important to consider the physical meaning of all of the included terms. It is not always clear when adding a term to a macroscopic model, how to translate this back to understand the physical implications of the choice. A further level of confidence in a macroscopic model is obtained when it can be derived from a microscopic one. In this case, the parameters of the microscopic

model may have a direct significance for the macroscopic model. Still one must be careful that this does not always imply that macroscopic phenomena correspond to the same calibration, and thorough comparison with data is needed. One must be aware that, when deriving a macroscopic model from a microscopic one, several assumptions have to be made from which the implications are not always fully understood. It is important to bear this in mind as derivations are undertaken.

On the other hand, if a microscopic model is being used, it can be very helpful, as in the case of (Alsenafi and Barbaro, 2018), to consider a macroscopic description of the model. While the theoretical analysis of the large number of differential equations involved in the microscopic models can become unwieldy, the tools accessible to analyze macroscopic equations are often well-developed, allowing for better predictions of the outcome from certain choices of parameter space. This is particularly true when modelling relies on game theory, when simulation and analysis become intractable in the case of a large number of agents, unless a mean-field assumption is done. It is therefore very helpful to consider if a corresponding macroscopic model can be derived when considering a microscopic model.

An interesting issue that we did not develop in this chapter is about calibration and validation of macroscopic models. A first level calibration is through the determination of the fundamental diagram (see Chap. 3), which as we have seen is at the core of first-order macroscopic models. Beyond that, macroscopic models could be directly calibrated or validated at the level of macroscopic phenomena such as wave propagation (Motsch et al., 2018), deformation of the density field (Butano et al., 2024a), etc. However, there is a need to go further in this direction and to develop more quantitative studies. Progress in the direct measurement of density through deep learning (Vandoni, 2019) could open possibilities for comparisons of macroscopic models with measurements in real events.

References

Aceves-Sánchez, P., Bailo, R., Degond, P., Mercier, Z., 2024. Pedestrian models with congestion effects. Math. Models Methods Appl. Sci. 34, 1001–1041. https://doi.org/10.1142/S0218202524400050.

Alisoltani, N., Ameli, M., Khoshyaran, M., Lebacque, J.-P., 2024. Mass evacuation planning based on mean field games theory. In: Rao, K., Seyfried, A., Schadschneider, A. (Eds.), Traffic and Granular Flow '22, Vol. 443 of Lecture Notes in Civil Engineering. Springer, Singapore, pp. 69–76. https://doi.org/10.1007/978-981-99-7976-9_9.

Alsenafi, A., Barbaro, A.B., 2018. A convection–diffusion model for gang territoriality. Phys. A: Stat. Mech. Appl. 510, 765–786. https://doi.org/10.1016/j.physa.2018.07.004.

Alsenafi, A., Barbaro, A.B., 2021. A multispecies cross-diffusion model for territorial development. Mathematics 9 (12), 1428. https://doi.org/10.3390/math9121428.

Amadori, D., Francesco, M.D., 2012. The one-dimensional Hughes model for pedestrian flow: Riemann—type solutions. Acta Math. Sci. 32, 259–280. https://doi.org/10.1016/S0252-9602(12)60016-2.

Amadori, D., Andreianov, B., Francesco, M.D., Fagioli, S., Girard, T., Goatin, P., Markowich, P., Pietschmann, J.-F., Rosini, M., Russo, G., Stivaletta, G., Wolfram, M., 2023. The mathematical theory of hughes' model: a survey of results. In: Bellomo, N., Gibelli, L. (Eds.), Crowd Dynamics, Volume 4: Analytics and Human Factors in Crowd Modeling. Springer International Publishing, Cham, pp. 9–53. https://doi.org/10.1007/978-3-031-46359-4_2.

Ameli, M., Faradonbeh, M., Lebacque, J.-P., Abouee-Mehrizi, H., Leclercq, L., 2022. Departure time choice models in urban transportation systems based on mean field games. Transp. Sci. 56, 1483–1504. https://doi.org/10.1287/trsc.2022.1147.

Andreianov, B., Donadello, C., Razafison, U., Rolland, J., Rosini, M., 2016. Solutions of the Aw-Rascle-Zhang system with point constraints. Netw. Heterog. Media 11, 29–47. https://doi.org/10.3934/nhm.2016.11.29.

Andreianov, B., Donadello, C., Razafison, U., Rosini, M., 2018. One-dimensional conservation laws with nonlocal point constraints on the flux. In: Gibelli, L., Bellomo, N. (Eds.), Crowd Dynamics, Volume 1: Theory, Models, and Safety Problems. Springer International Publishing, pp. 103–135. https://doi.org/10.1007/978-3-030-05129-7_5.

Andreianov, B., Donadello, C., Rosini, M., 2021. Entropy solutions for a two-phase transition model for vehicular traffic with metastable phase and time depending point constraint on the density flow. Nonlinear Differ. Equ. Appl. 28, 32. https://doi.org/10.1007/s00030-021-00689-5.

Andreianov, B., Rosini, M., Stivaletta, G., 2023. On existence, stability and many-particle approximation of solutions of 1d hughes' model with linear costs. J. Differ. Equ. 369, 253–298. https://doi.org/10.1016/j.jde.2023.06.004.

Appert-Rolland, C., Degond, P., Motsch, S., 2011. Two-way multi-lane traffic model for pedestrians in corridors. Netw. Heterog. Media 6, 351–381. https://doi.org/10.3934/nhm.2011.6.351.

Appert-Rolland, C., Pettré, J., Olivier, A.-H., Warren, W., Duigou-Majumdar, A., Pinsard, E., Nicolas, A., 2020. Experimental study of collective pedestrian dynamics. Collective Dyn. 5, 1–8. https://doi.org/10.17815/CD.2020.109.

Arechavaleta, G., Laumond, J.-P., Hicheur, H., Berthoz, A., 2008. An optimality principle governing human walking. IEEE Trans. Robot. 24, 5–14. https://doi.org/10.1109/TRO.2008.915449.

Aw, A., Rascle, M., 2000. Resurrection of "second order" models of traffic flow and numerical simulation. SIAM J. Appl. Math. 60, 916–938. https://doi.org/10.1137/S0036139997332099.

Aw, A., Klar, A., Materne, T., Rascle, M., 2002. Derivation of continuum traffic flow models from microscopic follow-the-leader models. SIAM J. Appl. Math. 63, 259–278. https://doi.org/10.1137/S0036139900380955.

Bürger, R., Goatin, P., Inzunza, D., Villada, L., 2020. A non-local pedestrian flow model accounting for anisotropic interactions and domain boundaries. Math. Biosci. Eng. 17, 5883–5906. https://doi.org/10.3934/mbe.2020314.

Bain, N., Bartolo, D., 2019. Dynamic response and hydrodynamics of polarized crowds. Science 363, 46. https://doi.org/10.1126/science.aat9891.

Barbaro, A.B., Chayes, L., D'Orsogna, M.R., 2013. Territorial developments based on graffiti: a statistical mechanics approach. Phys. A: Stat. Mech. Appl. 392 (1), 252–270. https://doi.org/10.1016/j.physa.2012.08.001.

Barbaro, A., Rodriguez, N., Yoldaş, H., Zamponi, N., 2021. Analysis of a cross-diffusion model for rival gangs interaction in a city. Commun. Math. Sci. 19, 2139–2175. https://doi.org/10.4310/CMS.2021.v19.n8.a4.

Benamou, J.-D., Carlier, G., Santambrogio, F., 2017. Variational mean field games. In: Bellomo, N., Degond, P., Tadmor, E. (Eds.), Active Particles, Volume 1: Advances in Theory, Models, and Applications. Springer, pp. 141–171. https://doi.org/10.1007/978-3-319-49996-3_4.

Berthelin, F., Degond, P., Delitala, M., Rascle, M., 2008. A model for the formation and evolution of traffic jams. Arch. Rational Mech. Anal. 187, 185–220. https://doi.org/10.1007/s00205-007-0061-9.

Bertozzi, A.L., Rosado, J., Short, M.B., Wang, L., 2015. Contagion shocks in one dimension. J. Stat. Phys. 158, 647–664. https://doi.org/10.1007/s10955-014-1019-6.

Blandin, S., Goatin, P., 2016. Well-posedness of a conservation law with non-local flux arising in traffic flow modeling. Numer. Math. 132, 217–241. https://doi.org/10.1007/s00211-015-0717-6.

Bonnemain, T., Gobron, T., Ullmo, D., 2020. Schrödinger approach to mean field games with negative coordination. SciPost Phys 9, 059. https://doi.org/10.21468/SciPostPhys.9.4.059.

Bonnemain, T., Butano, M., Bonnet, T., Echeverría-Huarte, I., Seguin, A., Nicolas, A., Appert-Rolland, C., Ullmo, D., 2023. Pedestrians in static crowds are not grains, but game players. Phys. Rev. E 107, 024612. https://doi.org/10.1103/PhysRevE.107.024612.

Bonnemain, T., 2020. Quadratic mean field games with negative coordination, Ph.D. thesis, Université Cergy-Pontoise. https://thibaultbonnemain.weebly.com/uploads/1/4/4/7/144795401/phd_thesis_thibault_bonnemain.pdf.

Bosse, T., Hoogendoorn, M., Klein, M., Treur, J., van der Wal, C., 2011. Agent-based analysis of patterns in crowd behaviour involving contagion of mental states. In: Mehrotra, K.G., Mohan, C.K., Oh, J.C., Varshney, P.K., Ali, M. (Eds.), Modern Approaches in Applied Intelligence. IEA/AIE 2011, Vol. 6704 of Lecture Notes in Computer Science. Springer, Berlin Heidelberg, pp. 566–577. https://doi.org/10.1007/978-3-642-21827-9_57.

Burger, M., Markowich, P., Pietschmann, J.-F., 2011. Continuous limit of a crowd motion and herding model: analysis and numerical simulations. Kinet. Relat. Mod. 4, 1025–1047. https://doi.org/10.3934/krm.2011.4.1025.

Burger, M., Francesco, M.D., Markowich, P., Wolfram, M.-T., 2014. Mean field games with nonlinear mobilities in pedestrian dynamics. Discrete Contin. Dyn. Syst. Ser. B 19, 1311–1333. https://doi.org/10.3934/dcdsb.2014.19.1311.

Burger, M., Göttlich, S., Jung, T., 2019. Derivation of second order traffic flow models with time delays. Netw. Heterog. Media 14, 265–288. https://doi.org/10.3934/nhm.2019011.

Burstedde, C., Klauck, K., Schadschneider, A., Zittartz, J., 2001. Simulation of pedestrian dynamics using a 2-dimensional cellular automaton. Phys. A 295, 507–525. https://doi.org/10.1016/S0378-4371(01)00141-8.

Butano, M., Appert-Rolland, C., Ullmo, D., 2024a. Discounted mean-field game model of a dense static crowd with variable information crossed by an intruder. SciPost Phys 16, 104. https://doi.org/10.21468/SciPostPhys.16.4.104.

Butano, M., Bonnemain, T., Appert-Rolland, C., Nicolas, A., Ullmo, D., 2024b. Modeling of obstacle avoidance by a dense crowd as a mean-field game. In: Rao, K., Seyfried, A., Schadschneider, A. (Eds.), Traffic and Granular Flow '22, Vol. 443 of Lecture Notes in Civil Engineering. Springer, Singapore, pp. 93–100. https://doi.org/10.1007/978-981-99-7976-9_6.

Campos, J., Corli, A., Malaguti, L., 2021. Saturated fronts in crowds dynamics. Adv. Nonlinear Stud. 21, 303–326. https://doi.org/10.1515/ans-2021-2118.

Canizo, J.A., Carrillo, J.A., Rosado, J., 2011. A well-posedness theory in measures for some kinetic models of collective motion. Math. Models Methods Appl. Sci. 21 (03), 515–539. https://doi.org/10.1142/S0218202511005131.

Carlini, E., Festa, A., Silva, F., Wolfram, M.-T., semi-Lagrangian, A., 2017. Scheme for a modified version of the Hughes' model for pedestrian flow. Dyn. Games Appl. 7, 683–705. https://doi.org/10.1007/s13235-016-0202-6.

Chalons, C., Goatin, P., Seguin, N., 2013. General constrained conservation laws. application to pedestrian flow modeling. Netw. Heterog. Media 8, 433–463. https://doi.org/10.3934/nhm.2013.8.433.

Chalons, C., 2007. Numerical approximation of a macroscopic model of pedestrian flows. SIAM J. Sci. Comput. 29 (2), 539–555. https://doi.org/10.1137/05064121.

Chaudhuri, N., Gwiazda, P., Zatorska, E., 2023. Analysis of the generalized Aw-Rascle model. Commun. Partial Differ. Equ. 48, 440–477. https://doi.org/10.1080/03605302.2023.2183511.

Chaudhuri, N., Feireisl, E., Zatorska, E., 2024a. Nonuniqueness of weak solutions to the dissipative Aw-Rascle model. Appl. Math. & Optim 90, 19. https://doi.org/10.1007/s00245-024-10158-x.

Chaudhuri, N., Navoret, L., Perrin, C., Zatorska, E., 2024b. Hard congestion limit of the dissipative Aw-Rascle system. Nonlinearity 37, 045018. https://doi.org/10.1088/1361-6544/ad2b14.

Chertock, A., 2017. A practical guide to deterministic particle methods. In: Handbook of Numerical Methods for Hyperbolic Problems, Vol. 18 of Handbook of Numerical Analysis. Elsevier, pp. 177–202. https://doi.org/10.1016/bs.hna.2016.11.004.

Chiarello, F., Friedrich, J., Goatin, P., Göttlich, S., 2020. Micro-macro limit of a nonlocal generalized Aw-Rascle type model. SIAM J. Appl. Math. 80, 1841–1861. https://doi.org/10.1137/20M1313337.

Chitour, Y., Jean, F., Mason, P., 2012. Optimal control models of goal-oriented human locomotion. SIAM J. Control Optim. 50, 147–170. https://doi.org/10.1137/100799344.

Cividini, J., Hilhorst, H., Appert-Rolland, C., 2013. Crossing pedestrian traffic flows, the diagonal stripe pattern and the chevron effect. J. Phys. A: Math. Theor 46, 345002. https://doi.org/10.1088/1751-8113/46/34/345002.

Colombo, R., Lécureux-Mercier, M., 2012. Nonlocal crowd dynamics models for several populations. Acta Math. Sci. 32, 177–196. https://doi.org/10.1016/S0252-9602(12)60011-3.

Colombo, R., Rosini, M., 2005. Pedestrian flows and non-classical shocks. Math. Meth. Appl. Sci. 28, 1553–1567. https://doi.org/10.1002/mma.624.

Colombo, R., Goatin, P., Maternini, G., Rosini, M., 2010. Macroscopic models for pedestrian flows. IUAV – TTL Research Unit (Ed.), Proceedings of the International Conference Big Events and Transport, Venice. pp. 11–22. https://inria.hal.science/inria-00534882.

Colombo, R., Herty, M., Mercier, M., 2011. Control of the continuity equation with a non local flow. ESAIM: Control, Optim. Calc. Var. 17, 353–379. https://doi.org/10.1051/cocv/2010007.

Colombo, R., Garavello, M., Lécureux-Mercier, M., 2012. A class of nonlocal models for pedestrian traffic. Math. Models Methods Appl. Sci. 22, 1150023. https://doi.org/10.1142/S0218202511500230.

Courant, R., Friedrichs, K., Lewy, H., 1928. Uber die partiellen differenzengleichungen der mathematischen physik. Mathematische Annalen 100, 32–74. https://doi.org/10.1007/BF01448839.

Cristiani, E., Piccoli, B., Tosin, A., 2014. Multiscale Modeling of Pedestrian Dynamics, Vol. 12 of MS&A. Springer. https://doi.org/10.1007/978-3-319-06620-2.

Cristiani, E., Priuli, F., Tosin, A., 2015. Modeling rationality to control self-organization of crowds: an environmental approach. SIAM J. on Applied Math 75, 605–629. https://doi.org/10.1137/140962413.

Cristiani, E., de Santo, A., Menci, M., 2023. A generalized mean-field game model for the dynamics of pedestrians with limited predictive abilities. Commun. Math. Sci. 21, 65–82. https://doi.org/10.4310/CMS.2023.v21.n1.a3.

Daganzo, C., 1995. Requiem for second-order fluid approximations of traffic flow. Transp. Res. B 29, 277–286. https://doi.org/10.1016/0191-2615(95)00007-Z.

Degond, P., Hua, J., Navoret, L., 2011. Numerical simulations of the euler system with congestion constraint. J. Comput. Phys. 230, 8057–8088. https://doi.org/10.1016/j.jcp.2011.07.010.

Degond, P., Appert-Rolland, C., Moussaid, M., Pettré, J., Theraulaz, G., 2013a. A hierarchy of heuristic-based models of crowd dynamics. J. Stat. Phys 152, 1033–1068. https://doi.org/10.1007/s10955-013-0805-x.

Degond, P., Appert-Rolland, C., Pettré, J., Theraulaz, G., 2013b. Vision-based macroscopic pedestrian models. Kinetic and Related Models 6, 809–839. https://doi.org/10.3934/krm.2013.6.809.

Degond, P., Liu, J.-G., Ringhofer, C., 2014. Large-scale dynamics of mean-field games driven by local Nash equilibria. J. Nonlinear Sci. 24, 93–115. https://doi.org/10.1007/s00332-013-9185-2.

Degond, P., 2004. Macroscopic limits of the boltzmann equation: a review. In: Degond, P., Pareschi, L., Russo, G. (Eds.), Modeling and Computational Methods for Kinetic Equations. Birkhäuser, Boston, Boston, MA, pp. 3–57. https://doi.org/10.1007/978-0-8176-8200-2_1.

Di Francesco, M., Markowich, P.A., Pietschmann, J.-F., Wolfram, M.-T., 2011. On the hughes' model for pedestrian flow: the one-dimensional case. J. of Diff. Equ. 250, 1334–1362. https://doi.org/10.1016/j.jde.2010.10.015.

Dogbé, C., 2008. On the numerical solutions of second order macroscopic models of pedestrian flows. Comput. Math. Appl. 56 (7), 1884–1898. https://doi.org/10.1016/j.camwa.2008.04.028.

Dogbé, C., 2011. Modeling crowd dynamics by the mean-field limit approach. Math. Comput. Model. 52, 1506–1520. https://doi.org/10.1016/j.mcm.2010.06.012.

Dogbé, C., 2012. On the modelling of crowd dynamics by generalized kinetic models. J. of Math. Analysis Applic 387, 512–532. https://doi.org/10.1016/j.jmaa.2011.09.007.

Duives, D., Daamen, W., Hoogendoorn, S., 2013. State-of-the-art crowd motion simulation models. Transp. Res. Part C: Emerg. Technol 37, 193–209. https://doi.org/10.1016/j.trc.2013.02.005.

Durupınar, F., 2010. From audiences to mobs: crowd simulation with sychological factors. Ph.D. thesis, Bilkent Universitesi (Turkey).

Etikyala, R., Göttlich, S., Klar, A., Tiwari, S., 2014. Particle methods for pedestrian flow models: from microscopic to nonlocal continuum models. Math. Models Methods Appl. Sci. 24 (12), 2503–2523. https://doi.org/10.1142/S0218202514500274.

Evans, L., 1998. Partial Differential Equations. 2nd Edition, Vol. 19 of Graduate Studies in Mathematics. American Mathematical Society.

Falcone, M., Ferretti, R., 2014. Semi-Lagrangian Approximation Schemes for Linear and Hamilton-Jacobi Equations. SIAM.

Fehrenbach, J., Narski, J., Hua, J., Lemercier, S., Jelić, A., Appert-Rolland, C., Donikian, S., Pettré, J., Degond, P., 2015. Time-delayed follow-the-leader model for pedestrians walking in line. Netw. Heterog. Media 10, 579–608. https://doi.org/10.3934/nhm.2015.10.579.

Feliciani, C., Corbetta, A., Haghani, M., Nishinari, K., 2023. Trends in crowd accidents based on an analysis of press reports. Saf. Sci. 164, 106174. https://doi.org/10.1016/j.ssci.2023.106174.

Francesco, M.D., Fagioli, S., Rosini, M., 2017. Deterministic particle approximation of scalar conservation laws. Boll. Unione Mat. Ital 10, 487–501. https://doi.org/10.1007/s40574-017-0132-2.

Goatin, P., Inzunza, D., Villada, L., 2024. Numerical comparison of nonlocal macroscopic models of multi-population pedestrian flows with anisotropic kernel. In: Parés, C., Castro, M.J., Morales de Luna, T., Muñoz-Ruiz, M.L. (Eds.), Hyperbolic Problems: Theory, Numerics, Applications. Volume II. HYP 2022, Vol. 35 of SEMA SIMAI Springer Series. Springer Nature Switzerland, Cham, pp. 371–381. https://doi.org/10.1007/978-3-031-55264-9_32.

Goatin, P., Inzunza, D., Villada, L., 2025. Nonlocal macroscopic models of multi-population pedestrian flows for walking facilities optimization. Appl. Math. Model. 141, 115927. https://doi.org/10.1016/j.apm.2025.115927.

Goatin, P., 2023. Macroscopic traffic flow modelling: from kinematic waves to autonomous vehicles. Commun. Appl. Ind. Math 14, 1–16. https://doi.org/10.2478/caim-2023-0001.

Gu, F., Guiselin, B., Bain, N., Zuriguel, I., Bartolo, D., 2025. Predicting and modeling emergent collective oscillations in massive crowds. Nature 638, 112–119. https://doi.org/10.1038/s41586-024-08514-6.

Guy, S., Curtis, S., Lin, M., Manocha, D., 2012. Least-effort trajectories lead to emergent crowd behaviors. Phys. Rev. E 85, 016110. https://doi.org/10.1103/PhysRevE.85.016110.

Haberman, R., 1998. Mathematical Models: Mechanical Vibrations, Population Dynamics, and Traffic Flow. SIAM. https://doi.org/10.1137/1.9781611971156.

Haghani, M., Coughlan, M., Crabb, B., Dierickx, A., Feliciani, C., van Gelder, R., Geoerg, P., Hocaoglu, N., Laws, S., Lovreglio, R., Miles, Z., Nicolas, A., O'Toole, W., Schaap, S., Semmens, T., Shahhoseini, Z., Spaaij, R., Tatrai, A., Webster, J., Wilson, A., 2023. A roadmap for the future of crowd safety research and practice: introducing the swiss cheese model of crowd safety and the imperative of a vision zero target. Saf. Sci. 168, 106292. https://doi.org/10.1016/j.ssci.2023.106292.

Harten, A., Engquist, B., Osher, S., Chakravarthy, S.R., 1997. Uniformly high order accurate essentially non-oscillatory schemes, III. J. Comput. Phys. 131 (1), 3–47. https://doi.org/10.1006/jcph.1996.5632.

Hartmann, D., von Sivers, I., 2013. Structured first order conservation models for pedestrian dynamics. Netw. Heterog. Media 8, 985–1007. https://doi.org/10.3934/nhm.2013.8.985.

Helbing, D., Johansson, A., Al-Abideen, H.Z., 2007. The dynamics of crowd disasters: an empirical study. Phys. Rev. E 75, 046109. https://doi.org/10.1103/PhysRevE.75.046109.

Herzog, R., Pietschmann, J., Winkler, M., 2023. Optimal control of Hughes' model for pedestrian flow via local attraction. Appl. Math. Optim 88, 87. https://doi.org/10.1007/s00245-023-10064-8.

Hoogendoorn, S., Bovy, P.H., 2000. Gas-kinetic modeling and simulation of pedestrian flows. Transp. Res. Rec. 1710 (1), 28–36. https://doi.org/10.3141/1710-04.

Hoogendoorn, S.P., Bovy, P.H.L., 2003. Simulation of pedestrian flows by optimal control and differential games. Optim. Control Appl. Meth 24, 153–172. https://doi.org/10.1002/oca.727.

Hoogendoorn, S.P., Bovy, P.H.L., 2004. Pedestrian route-choice and activity scheduling theory and models. Transp. Res. Part B: Methodol. 38, 169–190. https://doi.org/10.1016/S0191-2615(03)00007-9.

Hoogendoorn, S.P., van Wageningen-Kessels, F.L., Daamen, W., Duives, D.C., 2014. Continuum modelling of pedestrian flows: from microscopic principles to self-organised macroscopic phenomena. Phys. A: Stat. Mech. Appl. 416, 684–694. https://doi.org/10.1016/j.physa.2014.07.050.

Hoogendoorn, S., van Wageningen-Kessels, F., Daamen, W., Duives, D., Sarvi, M., 2015. Continuum theory for pedestrian traffic flow: local route choice modelling and its implications. Transp. Res. Proc. 7, 381–397. https://doi.org/10.1016/j.trpro.2015.06.020.

Huang, M., Malhamé, R., Caines, P., 2006. Large population stochastic dynamic games: closed-loop McKean-Vlasov systems and the Nash certainty equivalence principle. Commun Inf Syst 6, 221–252.

Huang, L., Wong, S., Zhang, M., Shu, C., Lam, W., 2009. Revisiting Hughes' dynamic continuum model for pedestrian flow and the development of an efficient solution algorithm. Transp. Res. Part B: Methodol. 43, 127–141. https://doi.org/10.1016/j.trb.2008.06.003.

Hughes, R., 2002. A continuum theory for the flow of pedestrians. Transp. Res. B 36, 507–535.

Jelić, A., Appert-Rolland, C., Lemercier, S., Pettré, J., 2012. Properties of pedestrians walking in line – fundamental diagrams. Phys. Rev. E 85, 036111. https://doi.org/10.1103/PhysRevE.85.036111.

Jiang, Y., Zhang, P., Wong, S., Liu, R., 2010. A higher-order macroscopic model for pedestrian flows. Phys. A: Stat. Mech. Appl 389, 4623–4635. https://doi.org/10.1016/j.physa.2010.05.003.

Jiang, Y.-Q., Guo, R.-Y., Tian, F.-B., Zhou, S.-G., 2016. Macroscopic modeling of pedestrian flow based on a second-order predictive dynamic model. Appl. Math. Model. 40, 9806–9820. https://doi.org/10.1016/j.apm.2016.06.041.

Jiang, Y.-Q., Hu, Y.-G., Huang, X., 2022. Modeling pedestrian flow through a bottleneck based on a second-order continuum model. Phys. A: Stat. Mech. Appl. 608, 128272. https://doi.org/10.1016/j.physa.2022.128272.

Kühne, R., 2011, Greenshields' legacy: highway traffic. In: Monograph Title: 75 Years of the Fundamental Diagram for Traffic Flow Theory: Greenshields Symposium, Transportation Research Board, 3–10.

Ketcheson, D., LeVeque, R., del Razo, M., 2020. Riemann Problems and Jupyter Solutions. SIAM 10.1137/1.9781611976212.

Khoshyaran, M., Lebacque, J.-P., 2024. Mean field games modeling for dynamic traffic assignment with information. In: Rao, K., Seyfried, A., Schadschneider, A. (Eds.), Traffic and Granular Flow '22, Vol. 443 of Lecture Notes in Civil Engineering. Springer, Singapore, pp. 463–470. https://doi.org/10.1007/978-981-99-7976-9_57.

Kirchner, A., Schadschneider, A., 2002. Simulation of evacuation processes using a bionics-inspired cellular automaton model for pedestrian dynamics. Phys. A 312, 260–276. https://doi.org/10.1016/S0378-4371(02)00857-9.

Lügering, H., Tepeli, D., Sieben, A., 2023. It's (not) just a matter of terminology: everyday understanding of "mass panic" and alternative terms. Saf. Sci. 163, 106123. https://doi.org/10.1016/j.ssci.2023.106123.

Lachapelle, A., Wolfram, M.-T., 2011. On a mean field game approach modeling congestion and aversion in pedestrian crowds. Transp. Res. Part B: Method 45, 1572–1589. https://doi.org/10.1016/j.trb.2011.07.011.

Lasry, J.-M., Lions, P.-L., 2006. Jeux à champ moyen. i - le cas stationnaire / mean field games. i - the stationary case. C. R. Acad. Sci. Paris, Ser. I 343, 619–625. https://doi.org/10.1016/j.crma.2006.09.019.

Lemercier, S., Jelic, A., Kulpa, R., Hua, J., Fehrenbach, J., Degond, P., Appert-Rolland, C., Donikian, S., Pettré, J., 2012. Realistic following behaviors for crowd simulation. Comput. Graph. Forum 31, 489–498. https://doi.org/10.1111/j.1467-8659.2012.03028.x.

LeVeque, R.J., 1992. Numerical Methods for Conservation Laws. vol. 24 Springer. https://doi.org/10.1007/978-3-0348-8629-1.

LeVeque, R.J., 2002. Finite Volume Methods for Hyperbolic Problems, Vol. 31 of Cambridge Texts in Applied Mathematics. Cambridge University Press. https://doi.org/10.1017/CBO9780511791253.

Lighthill, M., Whitham, G., 1955. On kinematic waves. II. A theory of traffic flow on long crowded roads. Proc. R. Soc. Lond. Seri. A, Math. Phys. Sci. A 229, 317–345. https://doi.org/10.1098/rspa.1955.0089.

Maity, S., Sundar, S., Kuhnert, J., 2024. A high-resolution meshfree particle method for numerical investigation of second-order macroscopic pedestrian flow models. Appl. Math. Model. 131, 205–232. https://doi.org/10.1016/j.apm.2024.03.024.

Maury, B., Roudneff-Chupin, A., Santambrogio, F., Venel, J., 2011. Handling congestion in crowd motion modeling. Netw. Heterog. Media 6, 485–519. https://doi.org/10.3934/nhm.2011.6.485.

Motsch, S., Moussaid, M., Guillot, E., Moreau, M., Pettré, J., Theraulaz, G., Appert-Rolland, C., Degond, P., 2018. Modeling crowd dynamics through coarse-grained data analysis. Math. Biosci. Eng. 15, 1271–1290. https://doi.org/10.3934/mbe.2018059.

Nicolas, A., Kuperman, M., Ibáñez, S., Bouzat, S., Appert-Rolland, C., 2019. Mechanical response of dense pedestrian crowds to the crossing of intruders. Sci. Rep. 9, 105. https://doi.org/10.1038/s41598-018-36711-7.

Payne, H., 1971. Models of freeway traffic and control. Simulation Councils Proc. Seri.: Math. Model Public Syst. 1, 51–60.

Piccoli, B., Tosin, A., 2009. Pedestrian flows in bounded domains with obstacles. Contin. Mech. Thermodyn. 21 (2), 85–107. https://doi.org/10.1007/s00161-009-0100-x.

Rio, K., Rhea, C., Warren, W., 2014. Follow the leader: visual control of speed in pedestrian following. J. Vision 14, 1–16. https://doi.org/10.1167/14.2.4.

Salam, P., Shamin, P., Bock, W., Klar, A., Tiwari, S., 2021. Disease contagion models coupled to crowd motion and mesh-free simulation. Math. Models Methods Appl. Sci. 31, 1277–1295. https://doi.org/10.1142/S0218202521400066.

Santo, E.D., Donadello, C., Pellegrino, S., Rosini, M., 2019. Representation of capacity drop at a road merge via point constraints in a first order traffic model. ESAIM: M2AN 53, 1–34. https://doi.org/10.1051/m2an/2019002.

Schadschneider, A., Kirchner, A., Nishinari, K., 2003. From ant trails to pedestrian dynamics. Appl. Bionics Biomech. 1, 11–19. https://doi.org/10.3233/ABB-2003-9693527.

Schadschneider, A., Chowdhury, D., Nishinari, K., 2011. Stochastic Transport in Complex Systems From Molecules to Vehicles. Elsevier.

Suchde, P., Jacquemin, T., Davydov, O., 2023. Point cloud generation for meshfree methods: an overview. Arch. Comput. Methods Eng. 30 (2), 889–915. https://doi.org/10.1007/s11831-022-09820-w.

Toll, W.V., Chatagnon, T., Braga, C., Solenthaler, B., Pettré, J., 2021. SPH crowds: agent-based crowd simulation up to extreme densities using fluid dynamics. Comput. & Graph. 98, 306–321. https://doi.org/10.1016/j.cag.2021.06.005.

Tordeux, A., Chraibi, M., Schadschneider, A., Seyfried, A., 2017. Influence of the number of predecessors in interaction within acceleration-based flow models. J. of Phys. A: Math. and Theo 50, 345102. https://doi.org/10.1088/1751-8121/aa7fca.

Tordeux, A., Costeseque, G., Herty, M., Seyfried, A., 2018. From traffic and pedestrian follow-the-leader models with reaction time to first order convection-diffusion flow models. SIAM J. Appl. Math. 78, 63–79. https://doi.org/10.1137/16M110695X.

Toro, E., 2009. Riemann Solvers and Numerical Methods for Fluid Dynamics: A Practical Introduction. Springer Verlag. https://doi.org/10.1007/b79761.

Tsai, J., Bowring, E., Marsella, S., Tambe, M., 2011. Empirical evaluation of computational emotional contagion models. In: Intelligent Virtual Agents, IVA 2011, Vol. 6895 of Lecture Notes in Computer Science. Springer, pp. 384–397. https://doi.org/10.1007/978-3-642-23974-8_42.

Twarogowska, M., Goatin, P., Duvigneau, R., 2013. Macroscopic modeling and simulations of room evacuation. Appl. Math. Model. 38, 5781–5795. https://doi.org/10.1016/j.apm.2014.03.027.

Ullmo, D., Swiecicki, I., Gobron, T., 2019. Quadratic mean field games. Phys. Rep. 799, 1–35. https://doi.org/10.1016/j.physrep.2019.01.001.

Vandoni, J., 2019. Ensemble methods for pedestrian detection in dense crowds. Ph.D. thesis, University Paris Saclay. https://theses.hal.science/tel-02318892.

Wang, L., Short, M.B., Bertozzi, A.L., 2017. Efficient numerical methods for multiscale crowd dynamics with emotional contagion. Math. Models Methods Appl. Sci. 27 (01), 205–230. https://doi.org/10.1142/S0218202517400073.

Whitham, G., 1974. Linear and Nonlinear Waves, Pure and Applied Math. Wiley-Interscience Monographs and Tracts, New York. https://doi.org/10.1002/9781118032954.

Xia, Y., Wong, S., Shu, C.-W., 2009. Dynamic continuum pedestrian flow model with memory effect. Phys. Rev. E 79, 066113. https://doi.org/10.1103/PhysRevE.79.066113.

Yuan, Y., Goñi-Ros, B., Bui, H., Daamen, W., Vu, H., Hoogendoorn, S., 2020. Macroscopic pedestrian flow simulation using Smoothed Particle Hydrodynamics (SPH). Transp. Res. Part C: Emer. Technol. 111, 334–351. https://doi.org/10.1016/j.trc.2019.12.017.

Zhang, H.M., 2002. A non-equilibrium traffic model devoid of gas-like behavior. Transp. Res. Part B: Methodol. 36, 275–290. https://doi.org/10.1016/S0191-2615(00)00050-3.

Zhang, H.M., 2003. Driver memory, traffic viscosity and a general viscous traffic flow model. Transp. Research Part B 37, 27–41. https://doi.org/10.1016/S0191-2615(01)00043-1.